Anonymous Referee #1

(Responses to the referee's comments are in bold)

This paper uses an extensive dataset of physical and biogeochemical observations to identify water source contributions to a unique Canadian fjord-type system and evaluate the results in relation to the fjord's air-sea CO_2 flux characteristics. Overall, I found this manuscript very well-written, with good explanations of methods used (with one exception I will discuss below), excellent descriptions of data analyses, and clear presentation of results. Also, the paper is concise!

We thank the referee for his(her) detailed and very positive comments.

While this is very welcome overall, the Introduction and Summary may actually benefit from some additional content. -The Introduction is a little light. Can more detail be added on coastal CO_2 emissions? While there may be little information on CO_2 emissions from fjord-like systems, there have certainly been studies on a variety of other coastal system types which might provide context for this study.

A few sentences will be added to the revised manuscript to summarize the current consensus about CO_2 emissions in estuarine and coastal environments, and the introduction will read:

"Anthropogenic emissions of carbon dioxide (CO_2) have propelled atmospheric CO_2 concentrations above the 410 ppm mark in 2019, the highest concentration recorded in the past 3 million years (Willeit et al., 2019). The oceans, the largest CO_2 reservoir on Earth, have taken up ca. 30% of the anthropogenic CO_2 emitted to the atmosphere since the beginning of the industrial era (Feely et al., 2004; Brewer and Peltzer, 2009; Doney et al., 2009; Orr, 2011, Le Quéré et al., 2012), mitigating the impact of this greenhouse gas on global warming (Sabine et al., 2004). On the other hand, the uptake of CO_2 by the oceans has led to modifications of the seawater carbonate chemistry and a decline in the average surface ocean pH by ~0.1 units since pre-industrial times, a phenomenon dubbed ocean acidification (Caldeira and Wickett, 2005). According to the Intergovernmental Panel on Climate Change (IPCC) "business as usual" emissions scenario IS92a and general circulation models, atmospheric CO_2 levels may reach 800 ppm by 2100, lowering the pH of the surface oceans by an additional 0.3-0.4 units, at a rate that is unprecedented in the geological record (Caldeira and Wickett, 2005; Hönisch et al., 2012; Rhein et al., 2013). The growing concern about the impacts of anthropogenic CO_2 emissions on climate as well as marine and terrestrial ecosystems calls for a meticulous quantification of organic and inorganic carbon fluxes, especially in coastal environments, including fjords, a major but poorly quantified component of the global carbon cycle and budget (Bauer et al., 2013; Najjar et al., 2018). Meaningful predictions of the effects of climate change on future fluxes are intricate given the very large uncertainty associated with present-day air-sea CO_2 flux estimates in coastal waters, including rivers, estuaries, tidal wetlands, and the continental shelf (Bauer et al., 2013; Najjar et al., 2018). The coastal ocean occupies only ~7% of the global ocean surface area, but plays a major role in biogeochemical cycles because it (1) receives massive inputs of terrestrial organic matter and nutrients through continental runoff and groundwater discharge; (2) exchanges matter and energy with the open ocean; and (3) is one of the most geochemically and biologically active areas of the biosphere, accounting for significant fractions of marine primary production (~14 to 30%), organic matter burial (~80%), sedimentary mineralization (~90%), and calcium carbonate deposition (~50%) (Gattuso et al., 1998).

Although the carbon cycle of the coastal ocean is acknowledged to be a major component of the global carbon cycle and budget, accurate quantification of organic and inorganic carbon cycling and fluxes in the coastal ocean — where land, ocean and atmosphere interact — remains challenging (Bauer et al., 2013; Najjar et al., 2018). Constraining the exchanges and fates of different forms of carbon along the land—ocean continuum is so far incomplete, owing to limited data coverage and large physical and biogeochemical variability within and between coastal subsystems (e.g., hydrological and geomorphological differences, differences in the magnitude and stoichiometry of organic matter inputs). Hence, owing to limited data coverage and suspicious upscaling due to the large physical and biogeochemical variability within and between coastal subsystems, there remains a debate as to whether coastal waters are net sources or sinks of atmospheric CO_2. Recent compilations of worldwide CO_2 partial pressure (pCO_2) measurements indicate that most open shelves in temperate and high-latitudes are sinks of atmospheric CO_2 whereas low-latitude shelves and most estuaries are sources (Chen and Borges, 2009; Cai, 2011; Chen et al., 2013). As noted by Bauer et al. (2013), estuaries are transitional aquatic environments that can be riverine or marine dominated and, thus, they typically display strong gradients in biogeochemical properties and processes as they flow seaward. Chen et al. (2013) reported that the strength of estuarine sources typically decreases with increasing salinity. However, marsh-dominated estuaries, in which active microbial decomposition of organic matter occurs in the intertidal zone, are strong sources of CO_2 (Cai, 2011).

High latitude waters such as the Arctic Ocean have recently been the foci of much research, while coastal, seasonally ice-covered aquatic environments, such as the Saguenay Fjord, that display comparable inter-annual and climatic sea-ice cover variabilities but are much more accessible, have been neglected (Bourgault et al., 2012). Characteristics of Arctic coastal ecosystems are found in the Saguenay Fjord, including the presence of many species of plankton, fish, birds and marine mammals as well as important freshwater inputs and the presence of seasonal ice cover (Bourgault et al., 2012). Fjords stand amongst the most productive ecosystems on the planet, while they have a yet unexplored role in regional and global carbon cycles as part of the estuarine family (Juul-Pedersen et al., 2015). They are crucial hotspots for organic carbon (mostly terrestrial) burial and account for nearly 11% of the annual organic carbon burial flux in marine sediments, while covering only 0.12% of oceans' surface (Rysgaard et al., 2012; Smith et al., 2015). In other words, organic carbon burial rates in fjords are a hundred times faster than the average rate in the global ocean. Rates of organic carbon burial provide insights on the mechanism that controls atmospheric O_2 and CO_2 concentrations over geological timescales (Smith et al., 2015).

This study presents 1) the relative contribution of known source waters to the water column in the fjord, estimated from the solution of an optimization multi-parameter algorithm (OMP) using geochemical and isotopic tracers, and 2) results of a conservative mixing model, based on results of the OMP analysis and from which theoretical surface-water pCO_2 values are derived and then compared to field measurements. The latter comparison serves to identify the dominant factors, other than physical mixing (i.e., biological activity, gas exchange), that impact the CO_2 fluxes at the air-sea interface throughout the fjord and modulate the trophic status of the fjord (i.e. whether it is a source or a sink of CO_2 to the atmosphere)."

References

Bauer, J. E., Cai, W. J., Raymond, P. A., Bianchi, T. S., Hopkinson, C. S., & Regnier, P. A. (2013) The changing carbon cycle of the coastal ocean. Nature, 504(7478), 61.

Bourgault, D., Galbraith, P. S., & Winkler, G. (2012) Exploratory observations of winter oceanographic conditions in the Saguenay Fjord. Atmosphere-Ocean, 50(1), 17-30.

Borges, A. V. (2005) Do we have enough pieces of the jigsaw to integrate CO_2 fluxes in the coastal ocean? Estuaries; Stony Brook, 28(1), 3–27. http://dx.doi.org/10.1007/BF02732750

Brewer, P. G., & Peltzer, E. T. (2009) Limits to marine life. Science, 324(5925), 347-348.

Cai, W.-J. (2011) Estuarine and coastal ocean carbon paradox: CO_2 sinks or sites of terrestrial carbon incineration? Annual Review of Marine Science, 3(1), 123–145. https://doi.org/10.1146/annurev-marine-120709-142723

Caldeira, K., & Wickett, M. E. (2005) Ocean model predictions of chemistry changes from carbon dioxide emissions to the atmosphere and ocean. Journal of Geophysical Research: Oceans, 110(C9).

Chen, C. T. A., & Borges, A. V. (2009) Reconciling opposing views on carbon cycling in the coastal ocean: Continental shelves as sinks and near-shore ecosystems as sources of atmospheric CO_2. Deep Sea Research Part II: Topical Studies in Oceanography, 56(8-10), 578-590.

Chen, C. T., Huang, T. H., Chen, Y. C., Bai, Y., He, X., & Kang, Y. (2013) Air–sea exchanges of CO_2 in the world's coastal seas. Biogeosciences, 10(10), 6509-6544.

Doney, S. C., Fabry, V. J., Feely, R. A., & Kleypas, J. A. (2009) Ocean acidification: the other CO_2 problem. Annual Review of Marine Science, 1, 169-192.

Gattuso, J.-P., Frankignoulle, M., and Wollast, R. (1998) Carbon and carbonate metabolism in coastal aquatic ecosystems. Annual Review of Ecology and Systematics, 29, 405–434.

Hönisch, B., Ridgwell, A., Schmidt, D. N., Thomas, E., Gibbs, S. J., Sluijs, A., ... & Kiessling, W. (2012) The geological record of ocean acidification. Science, 335(6072), 1058-1063.

Juul-Pedersen, T., Arendt, K., Mortensen, J., Blicher, M., Søgaard, D., and Rysgaard, S. (2015) Seasonal and interannual phytoplankton production in a sub-Arctic tidewater outlet glacier fjord, SW Greenland. Marine Ecology Progress Series, 524, 27–38. https://doi.org/10.3354/meps11174

Le Quéré, C., Andres, R. J., Boden, T., Conway, T., Houghton, R. A., House, J. I., ... & Andrew, R. M. (2012) The global carbon budget 1959–2011. Earth System Science Data Discussions, 5(2), 1107-1157.

Najjar R. G., Herrmann M., Alexander R., Boyer E. W., Burdige D. J., Butman D., Cai W. J.,Canuel E. A., Chen R. F., Friedrichs M. A. M., Feagin R. A., Griffith P. C., Hinson A. L.,Holmquist J. R., Hu X., Kemp W. M., Kroeger K. D., Mannino A., McCallister S. L.,McGillis W. R., Mulholland M. R., Pilskaln C. H., Salisbury J., Signorini S. R.,St-Laurent P., Tian H., Tzortziou M., Vlahos P., Wang Z. A. and Zimmerman R. C. (2018) Carbon budget of tidal wetlands, estuaries, and shelf waters of eastern North America. Global Biogeochemical Cycles, 32, 389–416.

Orr, J. C. (2011) Recent and future changes in ocean carbonate chemistry. Ocean Acidification, 1, 41-66.

Rhein, M., S.R. Rintoul, S. Aoki, E. Campos, D. Chambers, R.A. Feely, S. Gulev, G.C. Johnson, S.A. Josey, A. Kostianoy, C. Mauritzen, D. Roemmich, L.D. Talley and F. Wang, 2013: Observations: Ocean. In: Climate Change 2013: The Physical Science Basis. Contribution of Working Group I to the Fifth Assessment Report of the Intergovernmental Panel on Climate Change [Stocker, T.F., D. Qin, G.-K. Plattner, M. Tignor, S.K. Allen, J. Boschung, A. Nauels, Y. Xia, V. Bex and P.M. Midgley (eds.)]. Cambridge University Press, Cambridge, United Kingdom and New York, NY, USA.

Rysgaard, S., Mortensen, J., Juul-Pedersen, T., Sørensen, L. L., Lennert, K., Søgaard, D. H., … Bendtsen, J. (2012) High air–sea CO_2 uptake rates in nearshore and shelf areas of Southern Greenland: Temporal and spatial variability. Marine Chemistry, 128–129, 26–33.
https://doi.org/10.1016/j.marchem.2011.11.002

Sabine, C. L, (2004) The oceanic sink for anthropogenic CO_2. Science. 305(5682), 367–371. doi:10.1126/science.1097403.

Smith, R. W., Bianchi, T. S., Allison, M., Savage, C., and Galy, V. (2015) High rates of organic carbon burial in fjord sediments globally. Nature Geoscience, 8(6), 450–453.
https://doi.org/10.1038/ngeo2421

Willeit, M., Ganopolski, A., Calov, R., & Brovkin, V. (2019) Mid-Pleistocene transition in glacial cycles explained by declining CO_2 and regolith removal. Science Advances, 5(4), eaav7337.

-Similarly, the Summary and Conclusions section is pretty brief. At the very least, what do the authors see as the impacts of this work beyond the studied system? What future work might stem from these findings? –

A few sentences will be added to the revised manuscript to summarize the impacts of this work beyond the studied system, extend the conclusions of the data analysis to an understanding of the factors governing CO_2 fluxes at the air-water interface and how these might apply to other systems (regardless of scale).

"A study of the dissolved inorganic carbon budget of fjords not only affords information on their trophic status (i.e. source or sink of CO2 with respect to the atmosphere) and surface-water chemistry, but also provides insights on the magnitude of gas exchange and the amount of biological activity it sustains. In addition to biological production, upwelling, water temperature, and the spreading of freshwater plumes all regulate pCO2 in coastal systems. Wind speed is also critical as it impacts sea state and the efficiency of gas exchange at the air-sea interface (Chen et al., 2013). Hence, the importance of wind on controlling the CO2 flux needs to be further investigated, especially in high latitude fjords where strong winds are often focussed along narrow channels between steep cliffs and narrow inlets.
Anthropogenic activities, through climate change, are altering the continental water cycle, along with the flows of carbon, nutrients and sediment to the coastal oceans (Borges, 2005), and therefore, the sequestration of anthropogenic CO2 by the oceans. In glacial fjords, freshwater discharge will be modified by accelerated glacier melting and their ultimate demise. Knowledge of the spatial and temporal variability of glacial discharge and seasonal ice cover in high latitude fjords is essential to estimate their influence on circulation patterns and freshwater export, both of which impact local productivity, terrestrial carbon burial and export as well as CO2 fluxes in these complex ecosystems. Finally, an improved understanding of the coastal carbon cycle will require a more comprehensive

spatial and temporal coverage of surface mixed layer pCO2 data in these environments, ideally from direct measurements."

One very interesting finding of the paper is the negative Org-Alk of the Saguenay River and the fjord waters (Figure 2, manuscript lines 383-388). I am familiar with work detailing positive Org-Alk findings (i.e. calculated TA lower than that measured directly), but I can't think of another example of negative Org-Alk. Negative total alkalinity is common in very acidic waters, but the total alkalinity in this river is positive (although low). This implies to me that in the total alkalinity titration, there is some excess of acid that is not reflected in the pH and DIC measurements. What could this be? This leads me to wish there were more description of the TA measurement method. At which pH range was the titration carried out? What is a shallow end-point detection algorithm? Where might the excess acidity be coming from? A short discussion of the factors that could explain the negative Org-Alk would be a welcome addition.

The negative Org-Alk (acidity) component of this manuscript could make up a manuscript of its own and a detailed discussion is, therefore, beyond the scope of this study. For a discussion of the acid-base properties of dissolved organic matter in estuaries and the impact of OrgAlk on pH, acid-base dissociation and carbonic acid speciation, the reviewer should consult Cai et al. (1998) and Muller and Bleie (2008). Although positive values are most often reported, negative organic alkalinities (acidity) have been reported in coastal waters (e.g., Yang et al., 2015) and discussed (Ulfsbo et al., 2015). They are relatively common in rivers and stream waters of temperate regions where soil profiles are well developed and the bedrock is made up of crystalline rocks (igneous or metamorphic silicates) devoid of carbonates. In fact, all the rivers along the north shore of the St. Lawrence Estuary are characterized by circum-neutral pHs and negative Org-Alk (acidity) as they drain the metamorphic/igneous rocks of the Canadian Shield (Wilkinson et al., 1992). The negative Org-Alk (acidity) most likely originates from soil humic acids and all these rivers, including the Saguenay River, are highly colored. We added the following text to the revised manuscript:

"The negative Org-Alk (acidity) of the Saguenay River water most likely originates from soil humic acids that are flushed by percolation with groundwaters that drain the metamorphic and igneous rocks of the Canadian Shield."

Total alkalinity was measured by metered weak acid solution additions between pH 7 and 4, sometimes requiring flushing of the sample solution with N_2 to lower the pCO_2 and increase the initial pH. The shallow end-point detection algorithm is a proprietary software of the manufacturer, Radiometer, for weak acid/base potentiometric titration.

Cai W. J., Wang Y. and Hodson R. E. (1998) Acid-base properties of dissolved organic matter in the estuarine waters of Georgia, USA. Geochim. Cosmochim. Acta 62, 761 473–483

Muller F. L. L. and Bleie B. (2008) Estimating the organic acid contribution to coastal seawater alkalinity by potentiometric titrations in a closed cell. Anal. Chim. Acta 619, 183–191.

Ulfsbo A., Kuliński K., Anderson L. G. and Turner D. R. (2015) Modelling organic alkalinity in the Baltic Sea using a Humic-Pitzer approach. Mar. Chem. 168, 18–26.

Wilkinson K.J., Jones H.G., Campbell P.G.C. and Lachance M. (1992) Estimating organic acid contributions to surface water acidity in Quebec (Canada). Water, Air and Soil Pollution 61, 57-74.

Yang B., Byrne R.H. and Lindemuth M. (2015) Contributions of organic alkalinity to total alkalinity in coastal waters: A spectrophotometric approach. Mar. Chem. 176, 199-207.

-The air-sea CO_2 flux calculations were based on discrete measurements of DIC and pH at individual stations. However, to produce the overall fluxes for the system, the estuary must have been divided up spatially into segments, as implied by equation 5. However, these segments are not discussed or shown on the map (Figure 1), and should probably be included and delineated in the map.

The fjord was divided in segments based on the overall trend of the surface water pCO_2 ($pCO_{2(SW)}$) along the main axis of the fjord (Fig. 4): the first segment includes the larger inner basin (over which $pCO_{2(SW)}$ is much higher than $pCO_{2(air)}$ and decreases rapidly downstream) whereas the second segment encompasses the two outer basins (over which $pCO_{2(SW)}$ is close to $pCO_{2(air)}$ and varies little downstream). Segments will be identified on Figure 1.a.

-Also, pH data were important to this study, but are never shown. At the least it seems that the pH data should be shown in the Appendix figure, but really there should be a discussion of the pH findings before they are used to calculate pCO_2.

A table will be added to the Appendix with the raw pH data.

-In Figure 2, the SRW and CIL TA data are plotted against salinity. It's unclear to me where exactly these data were collected, or how they were selected. The SRW data fall into the salinity range of 0 to ~18 while the CIL data are saltier, from salinity ~22-35. A regression line is included (although I am skeptical of the R2 of 1.0 shown, given that there is at least some scatter in the data). However, to my eye it seems that the regression line of just the CIL data would produce a different (shallower) slope and (higher) y-intercept that that of the combined SRW and CIL data. If the CIL endmember TA:salinity regression were different, how would that affect the water mass mixing results?

R^2 = 0.999, which was rounded to 1 for ease of reference. It will be modified back to 0.999.

The reviewer is right (see below) in saying that the slope of the regression line to the CIL data is slightly shallower (TA/S_P = 47.8 vs 61.2) but the extrapolations to S_P = 0 (the SRW endmember) from the low salinity data (S_P < 11) alone are nearly identical (TA = 153 vs 147 µmol/kg). Hence, the water mass mixing results would not be affected significantly if the data were binned. The CIL definition was taken directly at the source of the endmember. As few data (0 < S_P < 5) were available to define the SRW, we used the full set of data from the fjord water column to correlate TA and S_P and extrapolate the definition of the SRW endmember to S_P = 0.

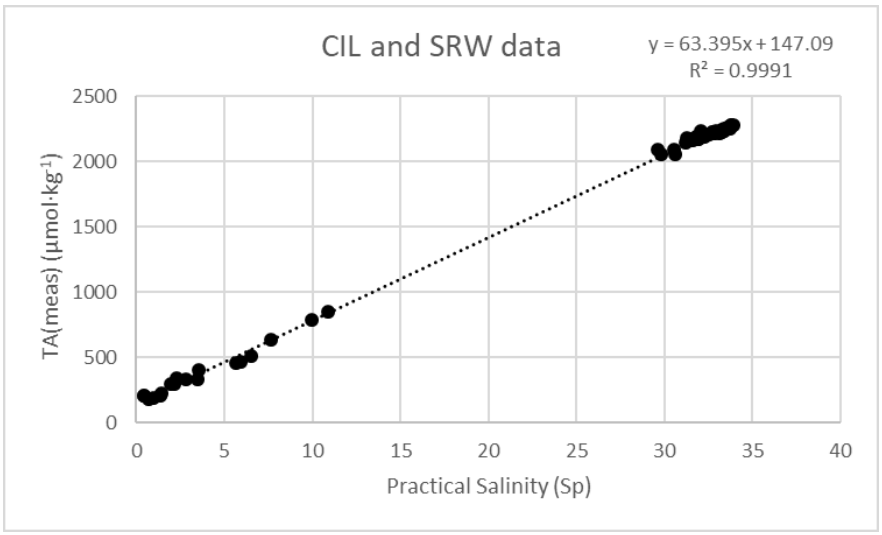
CIL and SRW data
y = 63.395x + 147.09
R² = 0.9991
TA(meas) (µmol·kg⁻¹)
Practical Salinity (Sp)
0
500
1000
1500
2000
2500
0
5
10
15
20
25
30
35
40

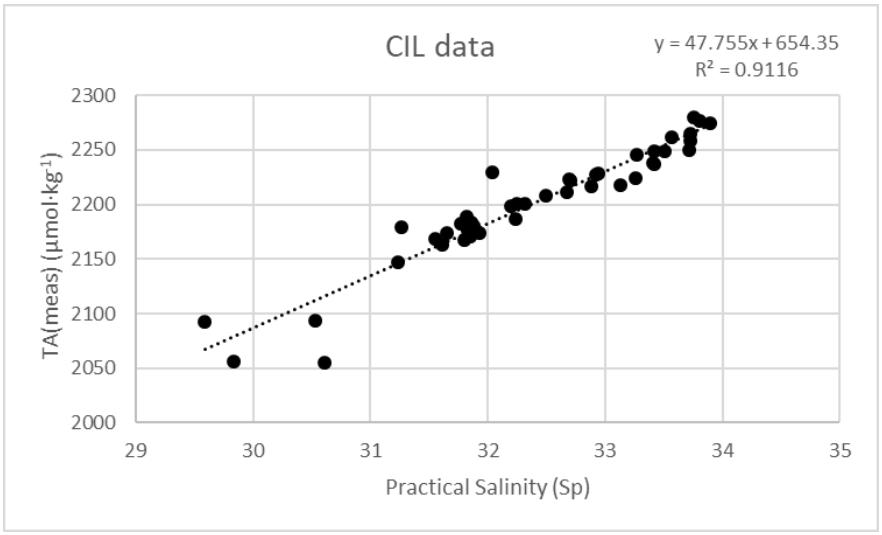
CIL data
y = 47.755x + 654.35
R² = 0.9116
TA(meas) (µmol·kg⁻¹)
Practical Salinity (Sp)
2000
2050
2100
2150
2200
2250
2300
29
30
31
32
33
34
35

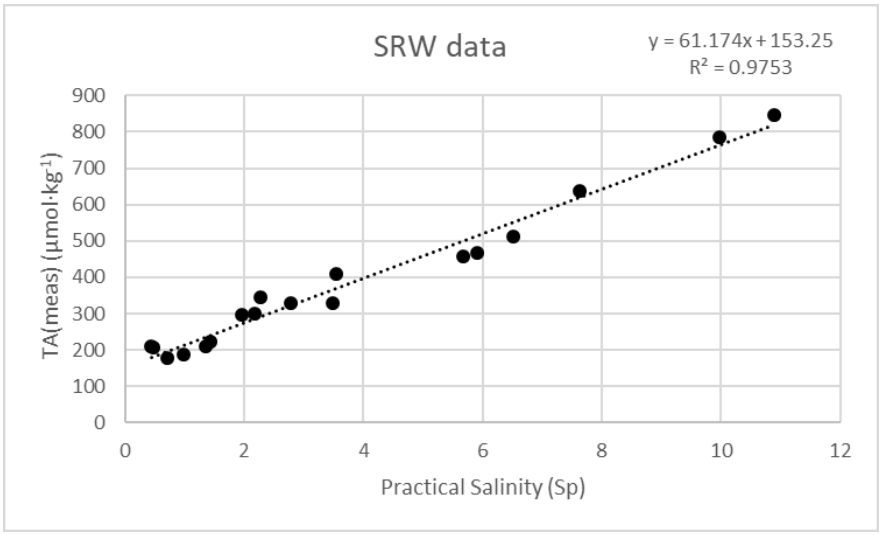
SRW data
y = 61.174x + 153.25
R² = 0.9753
TA(meas) (µmol·kg⁻¹)
Practical Salinity (Sp)
0
100
200
300
400
500
600
700
800
900
0
2
4
6
8
10
12

-L13-L15: this sentence is pretty awkward, can it be simplified?

The sentence will be simplified to ease understanding. In the revised manuscript, it will read:

"Nonetheless, the CO_2 dynamics in the fjord are modulated with the rising tide by the intrusion, at the surface, of brackish water from the upper estuary, as well as an overflow of mixed seawater over the shallow sill from the lower estuary."

-L26: is there a newer citation for atmospheric CO_2 levels than this 2008 work?

The other referee suggested Willeit et al (2019), which will be incorporated in the revised manuscript

- L77: the terms "Tmax" and "Sp" have not been defined

The terms will be defined in the revised manuscript. "Tmax" will be changed to "T", which stands for Temperature (in °C) whereas "S_P" refers to the practical salinity of the waters.

-L90: the St. Lawrence River and Estuary frequently appear in this manuscript, but it's unclear where these features begin and end in relation to the Saguenay system.

The original inset in Figure 1 will be replaced by the following map that also includes the location of sampling stations in the estuary and the gulf from which the SLR, CIL and LSLE endmember definitions were derived.

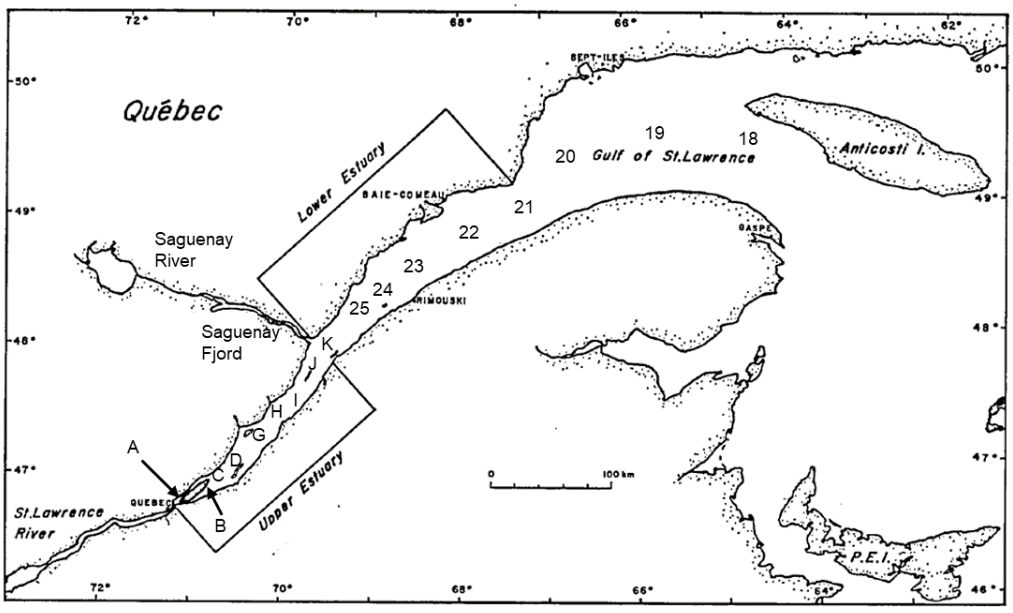

-L99: were samples from the St. Lawrence estuary included in the Appendix plot? There seem to be data in this plot that are quite different than those in Figure 2. If so, the locations of the St. Lawrence stations should be shown in Figure 1, and the difference between data from inside and outside the fjord should be clearer.

Samples from the St. Lawrence Estuary were included in the Appendix plot, specifically stations used to define endmembers other than the SRW. The location of sampling sites outside the fjord for which data are used in this plot will be identified in the new inset map (see above) and are identified by letters (A to K) in the Upper Estuary and numbers (18 to 25) in the Lower Estuary and the Gulf. The data taken inside and outside the fjord are distinguished by distinct symbols for each water mass.

-L110: what is the distinction between "TA" and "TA/DIC" samples?

"TA" refers to samples collected in 250 mL glass bottles throughout the water column and analyzed at McGill University. "TA/DIC" refers to surface water samples taken in 500 mL glass bottles and sent to Dalhousie University to be analysed by Dr. Helmuth Thomas for both TA and DIC. Methods, Lines 170-184 describe the analytical methods in detail.

-L124: what is "Rio Tinto Alcan"?

Rio Tinto Alcan is a large multinational aluminium smelter/producer. The company constructed and manages its own hydroelectric dam on the Saguenay River. We collaborated with a Water Management Consultant who provided us with freshwater discharge data as part of their bank stabilization programme.

-L275: can the location of the weather station be included on the map? What was the measurement height for the wind speed?

The weather station location will be included on the map. The weather station's elevation is 152 m above sea level.

-L276-277: this is a really nice, concise description of the Schmidt number

We thank the referee for his(her) positive comment

-L284: specify water temperature here

L284 will be rephrased in the revised manuscript and will read: "[…] where T is the temperature (°C) and A, B, C, D and E are fitting coefficients for seawater (S_P = 35) and freshwater (S_P =0), for water temperatures ranging from -2°C to 40°C (Wanninkhof, 2014)."

-L298: is there a way to cite or list the conversion formula from NOAA-NWS?

Unfortunately, we have not found a way of citing Tim Brice's (very useful!) work. However, a portable version of the Weather Calculator is now available (here)

-L336: How was the correction for organic alkalinity performed?

Line 320: "*The organic alkalinity of the fjord waters was estimated from the difference between the measured and calculated TA*". The organic alkalinity was then subtracted from TA_{meas} to give TA_{calc}.

-L414-424: this correlation analysis assumes that the sensor pCO_2 measurements are totally correct; however, there is a fair amount of uncertainty associated with these sensors. Error bars in both the x- and y-directions would be helpful in Figure 5.

As noted in the manuscript, "the manufacturer claims a 1% accuracy, but the performance of the instrument may be even better (Hunt et al., 2017)", an insignificant instrumental error. However, surface water pCO_2s recorded by the probe can vary by as much as 5% as the ship drifts from its position, water flows past the ship and probe, or waters are mixed by turbulence. Error bars will be added to Figure 5 in the revised manuscript.

-Figure 1: the color scale needs a label ('Salinity' etc)

The proper label will be added to Figure 1 in the revised manuscript.

-Figure 6(a): the line is dashed-black in my copy, not red as described in the caption

We thank the referee for catching this mistake! The figure caption will be modified accordingly in the revised manuscript.

-Figure 8: can the mean temperature used to normalize the data be listed somewhere in this figure, for ease of reference?

Temperatures used to normalize the data were listed on lines 430-432 of the original manuscript but will be listed in the figure caption for ease of reference.

Anonymous Referee #2

Coastal zones play an important hole on the global carbon cycling; however, carbon budges are not yet properly include in global carbon budgets. This paper presents a novel and integrative approach to estimate the relative contribution of known water sources to the Saguenay Fjord (Quebec, Canada), using geochemical and isotopic tracers coupled with an optimization multiparameter algorithm (OMP). This method, coupled with conservative end-member mixing model, allowed the analysis of dominant factors controlling the CO_2 dynamics in the Fjord. The paper is generally well-written and very easy to follow, providing new insights on coastal carbon dynamics. The paper is very succinct, and this is welcome. However, in some passages I would like to see more advances beyond the studied area. In brief, the manuscript lacks to present a better contextualization and to describe the implications of these findings. But of course this does diminish the merits of this manuscript. The introduction is too short. In recent years, the knowledge of CO_2 dynamics was considerable increased in coastal zones worldwide. In this way, I strongly recommend a review of the literature to contextualize your research.

We thank the referee for his(her) detailed and very positive comments.
A few sentences will be added to the revised manuscript to summarize the current consensus about CO_2 emissions in estuarine and coastal environments.

Please see response to Referee #1.

In addition, the discussion section is also very short, especially when discussing the governing processes that drive the concentrations and fluxes of CO_2 at the air-water interface in the estuary.

A few sentences will be added to the revised manuscript:

"These results highlight the importance of the freshwater plume from the Saguenay River in regulating the pCO_2 dynamics in the fjord. Winds, in addition to regulate the gas exchange coefficient, are also known to have a direct influence on air-sea CO_2 fluxes by driving upwelling of CO_2-rich waters along with the entrainment of nutrients in surface waters, thus increasing biological activity (Wanninkhof and Triñanes, 2017). However, wind speeds are relatively low in the studied system ($1.89\ m\ s^{-1} < u < 4.2\ m\ s^{-1}$, Table 2), implying a calm sea state (Frankignoulle, 1998), and hence reinforcing that changes in $pCO_{2(SW-SST)}$ can mainly be attributed to microbial respiration and photosynthesis modulated by water renewals rather than winds."

Frankignoulle, M. (1988) Field measurements of air-sea CO_2 exchange 1. Limnology and Oceanography, 33(3), 313-322.

Wanninkhof, R., and Triñanes, J. (2017) The impact of changing wind speeds on gas transfer and its effect on global air-sea CO_2 fluxes. Global Biogeochemical Cycles, 31(6), 961-974.

The methodology is overall well written; however I have some doubts especially about the OMP analysis. How did you weight "arbitrarily" the parameters included in the OMP calculations?
Coupled with specific comment: Lines 214-222: This passage is somewhat confuse. I think you should explain about this "arbitrary choices" in the weighting procedure based on covariance between tracers.

Parameters were weighted arbitrarily according to their mixing behaviors (i.e., whether they behave conservatively or not, are affected by biological activity or gas exchange across the air-water interface) following [Lansard, B., Mucci, A., Miller, L. A., Macdonald, R. W., and Gratton, Y.: Seasonal variability of water mass distribution in the southeastern Beaufort Sea determined by total alkalinity and $\delta^{18}O$, J. Geophys. Res-Oceans, 117, 2012.]. Furthermore, several OMP analyses were carried out using different weights for each parameter while always considering their conservative behavior (i.e., low, medium or high) and results were not affected significantly. To clarify, the following text will be added to the revised manuscript:
"Several OMP analyses were carried out using different weights for each parameter, while weighing their conservative behaviour appropriately (i.e., highly conservative vs. lightly conservative). Results were not affected significantly."

Another question: you argued, "Each source-water type is only appropriate for the fjord and for the period of study". The source-water type definitions were the Saguenay River (SWR), the St. Lawrence Estuary summertime Cold Intermediate Layer (CIL), the Lower St. Lawrence Estuary bottom waters (LSLE) and the St. Lawrence River (SLRW). The sampling campaigns were performed in late spring (May 2016 and May 2018), early summer (June 2017), and early and late fall (September 2014 and November 2017). I mean, the considered water masses encompass all characteristics of the sampled periods? Are there significant differences in the end-members considering these different seasons? Looking at the Appendix, there are some scattering in the end-members of SRW, CIL, SLRW and LSLE. Could this cause influences when calculating the OMP and the mixing model end-members?

A seasonality analysis was carried out in order to make sure the SWT definitions are appropriate for the period of study. Insignificant variations were observed in tracers such as ^{18}O, DIC, TA, DO and S_P. The only significantly variable tracer was T, which was given the lowest possible weight in the OMP analysis as to not skew the water mass analysis results.

We are currently writing a manuscript in which we tackle this issue in depth, including seasonal variations of bottom-water renewals in the fjord. It will include a thorough analysis of the seasonality of the SWT definitions.

The discussion of negative organic alkalinity should be better stressed in the manuscript. This is a very atypical pattern, taking into account that almost all studies that investigate organic alkalinity in coastal zones found positive concentrations.

As noted in our response to Reviewer#1's inquiry, negative organic alkalinities (acidity) in rivers are relatively common in temperate regions where soil profiles are well developed and the bedrock is made up of crystalline rocks (igneous or metamorphic silicates) devoid of carbonates. In fact, all the rivers along the north shore of the St. Lawrence Estuary are characterized by circum-neutral pHs and negative Org-Alk (acidity) as they drain the metamorphic/igneous rocks of the Canadian Shield. The negative Org-Alk (acidity) most likely originates from soil humic acids and all these rivers, including the Saguenay River, are highly colored.

Another point: How did you correct the values of TA (organic alkalinity) to compute the mixing models?

Line 320: "*The organic alkalinity of the fjord waters was estimated from the difference between the measured and calculated TA*". To avoid organic alkalinity skewing the results, TA was calculated (TA_{calc}) using DIC and pH. The corrected TA were then used in the mixing model.

Line 26 : As you are talking about the concentrations of CO_2 in the past, I recommend to include the study of Willeit et al (2019), which suggests that "the current CO_2 concentration is unprecedented over the past 3 million years".

We thank the referee for his(her) suggestion, as the other referee also recommended the use of a more recent reference.

Line 28: Here, I think the good reference is Feely et al. (2004).
Feely, R. A. 2004. Impact of Anthropogenic CO2 on the CaCO3 System in the Oceans. Science 305, 362.

The reference will be added to the revised manuscript.

Line 31: I could not find this reference. Is it Caldeira and Wickett (2005)?

Yes, it is. The in-text citation will be modified accordingly.

Line 38-40: This sentence is not clear.

The sentence will be simplified to ease understanding. It will read:

“High latitude waters such as the Arctic Ocean have recently been given most of the attention, while coastal, seasonally ice-covered aquatic environments, such as the Saguenay Fjord, display comparable inter-annual and climatic sea-ice cover variabilities all the while being much more accessible (Bourgault et al., 2012).”

Line 49: What do you refers to trophic status? According to Vollenweider et al. (1998), trophic conditions of marine waters are related to degree of nutrient enrichment. Oligotrophy means nutrient poor (low productivity) and eutrophy means nutrient rich (high productivity) waters. However, the analysis of trophic status “per se” do not give information whether the ecosystems is a source or a sink of CO_2 to the atmosphere.
Vollenweider, R. A., Giovanardi, F., Montanari, G., Rinaldi, A. 1998. Characterization of the trophic conditions of marine coastal waters with special reference to the NW Adriatic Sea: proposal for a trophic scale, turbidity and generalized water quality index. Environmetrics, 9, 329-357.

Trophic status is indeed directly linked to primary productivity and microbial respiration. In our definition of the trophic status, we differentiate between surface waters that are net sources and net sinks of CO_2 to the atmosphere. An autotrophic system will generally be a sink of CO_2 to the atmosphere whereas a heterotrophic system will generally be a source, but there might be exceptions in transition zones between CO_2-charged waters and productive estuarine waters.

Line 61: I could not find these tributaries in the Fig. 1b.

Tributaries will be added to Fig. 1a of the revised manuscript. We thank the referee for catching this mistake.

Lines 80-81: Please, give the range of temperature for the warm brackish surface layer of the St. Lawrence Estuary.

The range of temperatures for the warm brackish surface layer of the St. Lawrence Estuary will be added to the revised manuscript.

What is the tidal amplitude in the Fjord, and the longitudinal variations? Could you include this information?

The requested information will be added to the revised manuscript.

According to Seibert et al. (1979), the tidal amplitude at the mouth of the fjord near Tadoussac averages 4.0 m and increases slightly toward the head of the fjord (4.3 m near Port Alfred). Spring tides may reach an amplitude of 6 m.

Seibert, G. H., Trites, R. W., and Reid, S. J. (1979) Deepwater exchange processes in the Saguenay Fjord, J. Fish. Board Can., 36(1), 42– 53.

Lines 132-142: Why did you use different methodologies of pH measurements for Sp >5 (spectrophotometry) and Sp < 5 (potentiometric)? Did you investigate the differences between these methods?

The differences between these methods have been investigated by Mucci's research group over many cruises in the St. Lawrence Estuary and the Saguenay Fjord over the past 15 years. Low salinity waters (S_P < 5) are often colored, turbid and poorly buffered and, thus, are often not amenable to spectrophotometric measurements with colored dyes.

Lines 148-149: It no was clear how you did convert the pHNBS to pHT. Could you explain this procedure in the manuscript? Did you apply correction factors for the pH measurements at NBS scale for the TRIS buffer solutions (for which you have assigned the pHT)?

We calculated the difference between the assigned pH_T of a TRIS buffer of salinity close to the sample (±2.5) and the measured pH(NBS) of the TRIS buffer. The sample pH(NBS) was then converted to pH_T by subtracting this value from the measured pH(NBS) of the sample.

Line 158: What is the concentration of CO_2 that you insert in the vials?

99.998% pure CO_2 (Research Grade) was injected in dual inlet mode.

Line 189: ". . .biogeochemical cycling is imperative if one is to evaluate the movement of nutrients. . .". Something is missing here.

The sentence starts on line 188 and reads as follows: "Resolving the effects of mixing and biogeochemical cycling is imperative if one is to evaluate the transport of nutrients and tracers in a water body."

Lines 226-225: "In the context of biogeochemical cycles, a SWT should be defined where the water mass enters the basin, upstream from the mixing region (Karstensen, 2013)." However, if the water masses enter the basins downstream from the mixing region?

By "upstream from the mixing region", we mean before the SWT enters the mixing region, and therefore at the source of the SWT itself. The sentence will be reworded for clarity and will read:

"In the context of biogeochemical cycles, a SWT should be defined where the water mass enters the basin, before it enters the mixing region (Karstensen, 2013)."

Lines 229-233: You argued that "Each definition was captured relative to the fjord, i.e. each source-water type is only appropriate for the fjord and for the period of study". Are you sure that these chosen SWT are representative for the period of study (late spring, May 2016 and May 2018; early summer, June 2017; early and late fall, September 2014 and November 2017)?

A seasonality analysis was carried out in order to make sure the SWT definitions are appropriate for the period of study. Insignificant variations were observed in tracers such as $\delta^{18}O$, DIC, TA, DO and S_P. The only highly variable tracer was T, which was given the lowest possible weight in the OMP analysis.

In addition, did you take into account the seasonal variability of the end-members to calculate the OMP and the mixing models?

As noted above, there is insignificant seasonal variability when it comes to the SWT definitions.

Line 265: “F= -D $\delta c/\delta x$”. Provide the terms of the equation.

Terms of the equation will be defined in the revised manuscript:
F is the diffusion flux in mole sec^{-1} m^{-2}
D is the diffusion coefficient in m^2 sec^{-1}
C is the concentration of CO_2 in mole m^{-3}
x is the distance in m

Line 270: The parameterization of Wanninkhof (2014) is recommended for calculations of air-water exchanges in open ocean waters. I think you should include here other parameterization more appropriate for estuarine environments.

Dinauer and Mucci (2017) analyzed which parameterization was best in the context of the St. Lawrence Estuary system and the parametrization of Wanninkhof (2014) was deemed the most appropriate.

Line 305: It no is clear to me how you separated these segments for the fjord’s surface area. Did you separate by salinity? Distance from the mouth?

As noted in our response to Reviewer#1’s comment, the fjord was divided in segments based on the overall trend of the surface water pCO_2 ($pCO_{2(SW)}$) along the fjord (Fig. 4): the first segment includes the larger inner basin (over which $pCO_{2(SW)}$ is much higher than $pCO_{2(air)}$ and decreases rapidly downstream) whereas the second segment encompasses the two outer basins (over which $pCO_{2(SW)}$ is close to $pCO_{2(air)}$ and varies little downstream). Segments will be identified on Figure 1.a.

Lines 383-385: The discussion of the negative organic alkalinity results are poorly presented. I recommend put more efforts in this subject.

See above for response to Reviewer#1’s comment.

Lines 414-420: You attributed the average difference between pCO_2(SW-meas) and pCO_2(SW-calc) to the uncertain associated with the carbonic acid dissociation constants. One possible alternative is to calculate the pCO_2(SW-calc) using other available constants to investigate which one fits better with the pCO_2(SW-meas).

Dinauer and Mucci (2017) investigated which set of carbonic acid dissociation constants returned the most realistic values of pCO_2 in the St. Lawrence Estuary system, which is why the constants from Cai and Wang (1998) were used in this study. As reported in Dinauer and Mucci (2017) other sets of constants return pCO_2(SW-calc) values that differ by as much as ± 300 ppm at salinities below 5.

Lines 435-446: This paragraph is very interesting, but I missed the comparison with other studies that applied end-member mixing models, contrasting the influences of mixing and biological activities.

We kindly suggest the referee have a look at the following studies:

Dinauer, A., and Mucci, A. (2017). Spatial variability in surface-water pCO_2 and gas exchange in the world's largest semi-enclosed estuarine system: St. Lawrence Estuary (Canada). Biogeosciences, 14(13), 3221-3237.

Dinauer, A., and Mucci, A. (2018). Distinguishing between physical and biological controls on the spatial variability of pCO_2: A novel approach using OMP water mass analysis (St. Lawrence, Canada). Marine Chemistry, 204, 107-120.

Lines 447-457: Where are the results of the fluorometer? I think this section can be strengthened adding with these results. For example you argued that "Additionally, it is interesting to note that NDIC is chronically negative for all sampling months near the 45 km mark." Maybe the fluorescence call tell something.

We thank the referee for his/her suggestion. We used the CTD profiles from 2014 and 2016 (since the mixing responses are different between these two years) but the fluorescence data do not reveal any significant chronic change that could explain the negative ΔNDIC at the 45 km mark (red line).

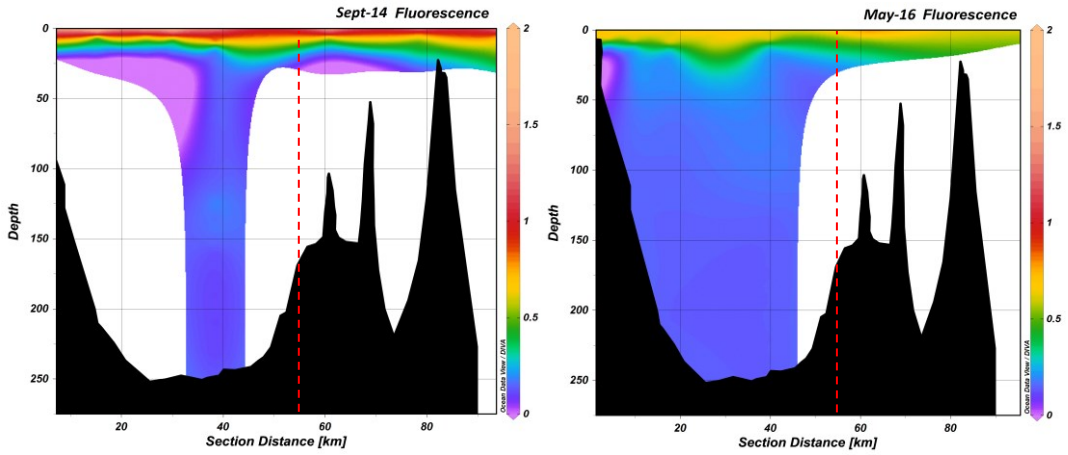

Fig. 1b. Please, provide the title of the Y-right axis. In addition, add the riverine positions in the figure and the estuarine sections you used to calculate the air-water CO_2 fluxes.

The requested information will be added in the revised manuscript.

Fig. 10. Normally, the comparison of DIC and AOU are performed by calculating the excess of dissolved inorganic carbon (E-DIC), which is difference between the in situ DIC and a theoretical DIC at atmospheric equilibrium. Are there differences comparing ΔNDIC x AOU with E-DIC x AOU?

It is true that calculating E-DIC is a more conventional way of plotting these data. Nevertheless, there appears to be no notable difference between ΔNDIC x AOU and E-DIC x AOU except for May 2016. This, however, does not change the conclusion of the manuscript given that our focus is on how ΔNDIC changes spatially.

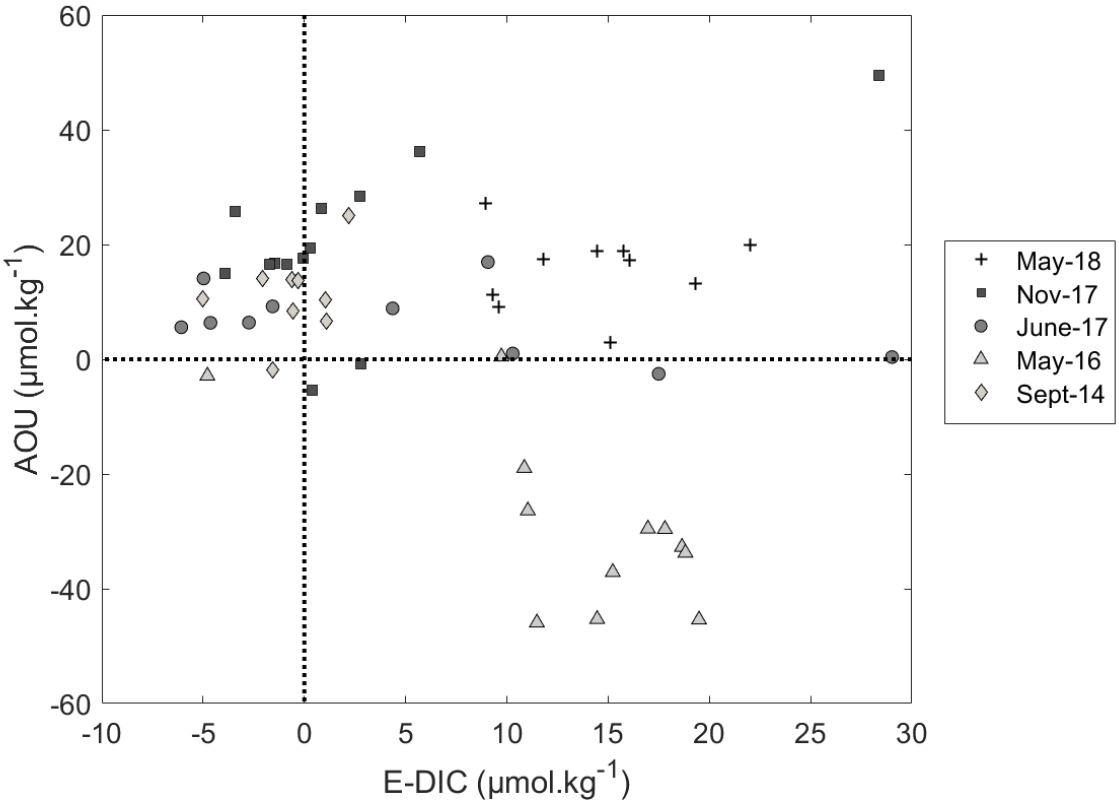
60
40
20
0
-20
-40
-60
-10
-5
0
5
10
15
20
25
30
AOU (µmol.kg-1)
E-DIC (µmol.kg-1)
May-18
Nov-17
June-17
May-16
Sept-14

List of all relevant changes made in the manuscript

(Line numbers refer to the revised manuscript)

TEXT

- A few sentences were added to the revised Introduction, further summarizing the current consensus about CO_2 emissions in estuarine and costal environments;
- A few sentences were added to the revised Summary and Conclusions to summarize the impacts of this work beyond the studied system, extend the conclusions of the data analysis to an understanding of the factors governing CO_2 fluxes at the air-water interface and how these might apply to other systems (regardless of scale);
- A few sentences were added to the revised Discussion, further discussing the governing processes that drive the concentrations and fluxes of CO_2 at the air-water interface in the estuary;

- L426-428: A sentence was added, highlighting the factors behind the negative Org-Alk of the Saguenay River water;
- L13-15: A sentence was modified for ease of understanding;
- L110-111: Term $T_{max\_}$ was changed to T, standing for Temperature (in °C). Both T and S_P were defined then (earlier than in first submission), as requested;
- L157-158: A description of Rio Tinto Alcan was added;
- L323: The word "water" was added, so the sentence now reads: "[…] where T is the temperature
- (°C) and A, B, C, D and E are fitting coefficients for seawater (SP = 35) and freshwater (SP
- =0), for **water** temperatures ranging from -2°C to 40°C (Wanninkhof, 2014).";
- L255-257: two sentences were added to clarify arbitrary choices made in running OMP calculations;
- L32: The reference Caldeira (2005) was modified to Caldeira and Wickett (2005);
- L113-114: The range of temperatures for the warm brackish surface layer of the St. Lawrence Estuary were added;
- L99-101: The tidal amplitude of the fjord and longitudinal variations were added to the fjord's description;
- L192: The concentration of CO_2 inserted in the vials was added;
- L261-262: The sentence was modified for ease of understanding;
- L303-304: Terms of the equation were provided.

FIGURES

- Figure 1:
    - Fjord segments were identified in Fig. 1.a;
    - The weather station location was added on Fig. 1.a;
    - The original inset in Fig. 1.a was replaced by another map which includes the location of sampling stations in the estuary and the gulf from which the SLR, CIL and LSLE endmember definitions were derived;

    - The color scale label ("Practical Salinity (S_P)") was added to Fig. 1.b;
    - Tributaries were added to Fig. 1.a;
    - Riverine positions and estuarine sections used to calculate the air-water CO_2 fluxes were added to Fig. 1.a (see inset).
- Figure 2: R^2 was modified to 0.999 (instead of 1);
- Figure 5: Error bars were added (smaller than the symbol);
- Figure 6: The caption was modified as line is dashed-black;
- Figure 8: Temperatures used to normalize the data were listed in the figure caption for ease of reference;
- A table was added to the Appendix with the raw pH data.

REFERENCES

- As requested, reference Willet et al. (2019) was incorporated in the Introduction [Willeit, M., Ganopolski, A., Calov, R., & Brovkin, V. (2019) Mid-Pleistocene transition in glacial cycles explained by declining CO2 and regolith removal. Science Advances, 5(4), eaav7337];
- As requested, reference Feely et al. (2004) was incorporated in the Introduction [Feely, R. A. 2004. Impact of Anthropogenic CO_2 on the $CaCO_3$ System in the Oceans. Science 305, 362];
- L31: the in-text citation Caldeira (2005) was modified to Caldeira and Wickett (2005).

Spatial variations of CO_2 fluxes in the Saguenay Fjord (Québec, Canada) and results of a water mixing model

Louise Delaigue[1], Helmuth Thomas[2,3] and Alfonso Mucci[1]
[1]GEOTOP and Department of Earth and Planetary Sciences, McGill University, 3450 University Street, Montreal, QC H3A 0E8, Canada
[2]Department of Oceanography, Dalhousie University, Halifax, Nova Scotia, Canada ~~(now at Center for Materials and Coastal Research, Helmholtz-Zentrum Geesthacht, Germany)~~
[3]Center for Materials and Coastal Research, Helmholtz-Zentrum Geesthacht, Germany

Correspondence to: Louise Delaigue (louise.delaigue@mail.mcgill.ca)

Abstract. The Saguenay Fjord is a major tributary of the St. Lawrence Estuary and is strongly stratified. A 6-8 m wedge of brackish water typically overlies up to 270 m of seawater. Relative to the St. Lawrence River, the surface waters of the Saguenay Fjord are less alkaline and host higher dissolved organic carbon (DOC) concentrations. In view of the latter, surface waters of the fjord are expected to be a net source of CO_2 to the atmosphere, as they partly originate from the flushing of organic-rich soil porewaters. Nonetheless, the CO_2 dynamics in the fjord are modulated with the rising tide by the intrusion, at the surface, of brackish water from the ~~upper estuary with the rising tide~~Upper St. Lawrence Estuary, as well as ~~mixing~~an overflow of mixed seawater~~, overflowing over~~ the shallow sill from the ~~lower estuary, modulate the CO_2 dynamics in the fjord.~~Lower St. Lawrence Estuary. Using geochemical and isotopic tracers, in combination with an optimization ~~multiparameter~~multi-parameter algorithm (OMP), we determined the relative contribution of known source-waters to the water column in the Saguenay Fjord, including waters that originate from the Lower St. Lawrence Estuary and replenish the fjord's deep basins. These results, when combined to a conservative mixing model and compared to field measurements, serve to identify the dominant factors, other than physical mixing, such as biological activity (photosynthesis, respiration) and gas exchange at the air-water interface, that impact the water properties (e.g., pH, pCO_2) of the fjord. Results indicate that the fjord's surface waters are a net source of CO_2 to the atmosphere during periods of high freshwater discharge (e.g., spring freshet) whereas they serve as a net sink of atmospheric CO_2 when their practical salinity exceeds ~ 5-10.

1 Introduction

Anthropogenic emissions of carbon dioxide (CO_2) have recently propelled atmospheric CO_2 concentrations above the 410 ppm mark, the highest concentration recorded in the past ~~800,000~~3 million years (~~Lüthi~~Willeit et al., ~~2008~~2019). The oceans, the largest CO_2 reservoir on Earth, have taken up ca. 30% of the anthropogenic CO_2 emitted to the atmosphere since the beginning of the industrial era (Feely et al., 2004; Brewer and Peltzer, 2009; Doney et al., 2009; Orr, 2011, Le Quéré et al., 2012), mitigating the impact of this greenhouse gas on global warming ~~-~~ (Sabine et al., 2004). On the other hand, the uptake of CO_2 by the oceans has led to modifications of the seawater carbonate chemistry and a decline in the average surface ocean pH by ~0.1 units since pre-industrial times, a phenomenon dubbed ocean acidification (Caldeira and Wickett, 2005). According to the Intergovernmental Panel on Climate Change (IPCC) "business as usual" emissions scenario IS92a and general circulation models, atmospheric CO_2 levels

Formatted: English (United Kingdom)
Formatted: English (United Kingdom)
Formatted: English (United Kingdom)
Formatted: English (United Kingdom)
Formatted: English (United Kingdom)
Formatted: English (United Kingdom)
Formatted: English (United Kingdom)
Formatted: English (United Kingdom)
Formatted: English (United Kingdom)
Formatted: English (United Kingdom)
Formatted: English (United Kingdom)
Formatted: English (United Kingdom)
Formatted: English (United Kingdom)

may reach 800 ppm by 2100, lowering the pH of the surface oceans by an additional 0.3-0.4 units, ~~-~~at a rate that is unprecedented in the geological record (Caldeira and Wickett, 2005; Hönisch et al., 2012; Rhein et al., 2013). The growing concern about the impacts of anthropogenic CO_2 emissions on climate as well as marine and terrestrial ecosystems calls for a meticulous quantification of organic and inorganic carbon fluxes, especially in coastal environments, including fjords, a major but poorly quantified component of the global carbon cycle and budget (Bauer et al., 2013~~). While much attention has recently focused~~; Najjar et al., 2018). Meaningful predictions of the effects of climate change on ~~high latitude~~ future fluxes are intricate given the very large uncertainty associated with present-day air-sea CO_2 flux estimates in coastal waters, including rivers, estuaries, tidal wetlands, and the continental shelf (Bauer et al., 2013; Najjar et al., 2018). The coastal ocean occupies only ~7% of the global ocean surface area, but plays a major role in biogeochemical cycles because it (1) receives massive inputs of terrestrial organic matter and nutrients through continental runoff and groundwater discharge; (2) exchanges matter and energy with the open ocean; and (3) is one of the most geochemically and biologically active areas of the biosphere, accounting for significant fractions of marine primary production (~14 to 30%), organic matter burial (~80%), sedimentary mineralization (~90%), and calcium carbonate deposition (~50%) (Gattuso et al., 1998).

Although the carbon cycle of the coastal ocean is acknowledged to be a major component of the global carbon cycle and budget, accurate quantification of organic and inorganic carbon cycling and fluxes in the coastal ocean — where land, ocean and atmosphere interact — remains challenging (Bauer et al., 2013; Najjar et al., 2018). Constraining the exchanges and fates of different forms of carbon along the land—ocean continuum is so far incomplete, owing to limited data coverage and large physical and biogeochemical variability within and between coastal subsystems, (e.g., hydrological and geomorphological differences, differences in the magnitude and stoichiometry of organic matter inputs). Hence, owing to limited data coverage and suspicious upscaling due to the large physical and biogeochemical variability within and between coastal subsystems, there remains a debate as to whether coastal waters are net sources or sinks of atmospheric CO_2. Recent compilations of worldwide CO_2 partial pressure (pCO_2) measurements indicate that most open shelves in temperate and high-latitudes are sinks of atmospheric CO_2 whereas low-latitude shelves and most estuaries are sources (Chen and Borges, 2009; Cai, 2011; Chen et al., 2013). As noted by Bauer et al. (2013), estuaries are transitional aquatic environments that can be riverine or marine dominated and, thus, they typically display strong gradients in biogeochemical properties and processes as they flow seaward. Chen et al. (2013) reported that the strength of estuarine sources typically decreases with increasing salinity. However, marsh-dominated estuaries, in which active microbial decomposition of organic matter occurs in the intertidal zone, are strong sources of CO_2 (Cai, 2011).

High latitude waters such as the Arctic Ocean~~),~~ have recently been the foci of much research, while coastal, seasonally ice-covered aquatic environments, such as the Saguenay Fjord ~~have displayed~~, that display comparable inter-annual and climatic sea-ice cover variabilities but are much more accessible, have been neglected (Bourgault et al., 2012). Characteristics of Arctic coastal ecosystems are found in the Saguenay Fjord, including the presence of many species of plankton, fish, birds and marine mammals as well as important freshwater inputs and the presence of seasonal ice cover (Bourgault et al., 2012). Fjords stand amongst the most productive ecosystems on the planet, while they have a yet unexplored role in regional and global carbon cycles as part of the estuarine family (Juul-

Formatted: English (United Kingdom)
Formatted: English (United Kingdom)
Formatted: English (United Kingdom)
Formatted: English (United Kingdom)
Formatted: English (United Kingdom)
Formatted: No Spacing, Line spacing: 1.5 lines
Formatted: Font: 10 pt, English (United States)
Formatted: Font: 10 pt, English (United States)
Formatted: Font: 10 pt, English (United States)
Formatted: Font: 10 pt, English (United States)
Formatted: Font: Times New Roman, 10 pt, English (United States)

Pedersen et al., 2015). They are crucial hotspots for organic carbon (mostly terrestrial) burial and account for nearly 11% of the annual organic carbon burial flux in marine sediments, while covering only 0.12% of oceans' surface (Rysgaard et al., 2012; Smith et al., 2015). In other words, organic carbon burial rates in fjords are a hundred times faster than the average rate in the global ocean. Rates of organic carbon burial provide insights on the mechanism that controls atmospheric O_2 and CO_2 concentrations over geological timescales (Smith et al., 2015).

This study presents 1) the relative contribution of known source waters to the water column in the fjord, estimated from the solution of an optimization ~~multiparameter~~multi-parameter algorithm (OMP) using geochemical and isotopic tracers, and 2) results of a conservative mixing model, based on results of the OMP analysis and from which theoretical surface-water pCO_2 values are derived and then compared to field measurements. The latter comparison serves to identify the dominant factors, other than physical mixing (i.e. biological activity, gas exchange), that impact the CO_2 fluxes at the air-sea interface throughout the fjord and modulate the trophic status of the fjord (i.e. whether it is a source or a sink of CO_2 to the atmosphere).

Formatted: Font: Times New Roman, 10 pt, Not Bold, English (United States)

Formatted: Indent: First line: 1.27 cm

Formatted: English (United Kingdom)

Formatted: English (United Kingdom)

Formatted: English (United Kingdom)

Formatted: Font: Not Bold

2 Data and methods

2.1 Study site characteristics

Located in the subarctic region of Québec, eastern Canada, the Saguenay Fjord is up to 275 m deep, 110 km long and has an average width of 2 km, with a 1.1 km wide mouth where it connects to the head of the Lower St. Lawrence Estuary (Fig. 1.a). The fjord's bathymetry includes three basins bound by three sills (Fig. 1.b). The first one, at a depth of ~20 m, is located at its mouth near Tadoussac and controls the overall dynamics of the fjord. The second is located 18 km further upstream and sits at a depth of 60 m, while the third one is found another 32 km further upstream and rises to a depth of 115 m. The fjord's drainage basin is 78,000 km^2 and is part of the greater St. Lawrence drainage basin (Smith and Walton, 1980), forming a hydrographic system, along with the Great Lakes, of more than 1.36 million km^2.

Tributaries to the Saguenay Fjord include the Saguenay, Éternité and Sainte-Marguerite Rivers (Fig. 1.~~b~~a). The Saguenay River is the main outlet from the Saint-Jean Lake, and flows into the North Arm of the fjord near St. Fulgence (Fig. 1.~~b~~a) with a mean freshwater discharge of ~1200 $m^3\ s^{-1}$ (Bélanger, 2003). Two other local, minor tributaries, the Rivière-à-Mars (95 km long, mean discharge ~8 $m^3\ s^{-1}$) and the Rivière des Ha! Ha! (35 km long, mean discharge ~15 $m^3\ s^{-1}$) discharge into the Baie des Ha! Ha!, a distinct feature of the Saguenay Fjord. (Fig. 1.a). Finally, the fjord receives denser marine waters from the St. Lawrence Estuary, filling the bottom of the three basins, as these waters episodically overflow the entrance sill (Therriault and Lacroix, 1975; Stacey and Gratton, 2001; Bélanger, 2003; Belzile et al., 2016). According to Seibert et al. (1979), the tidal amplitude at the mouth of the fjord near Tadoussac averages 4.0 m and increases slightly toward the head of the fjord (4.3 m near Port Alfred). Spring tides may reach an amplitude of 6 m.

The overflow and the intrusion of marine waters from the St. Lawrence Estuary generate a sharp halocline, leading to a simplified two-layer stratification in the fjord (Fig 1.b). The tidally-modulated intrusion of marine waters from the St. Lawrence Estuary into the Saguenay Fjord, as well as the outflow of the fjord into the estuary, have a

major influence on the water column stratification and circulation in the Saguenay Fjord and at its mouth (Belzile et al., 2016; Mucci et al., ~~20182~~2017). In other words, the properties of the uppermost 100 m of the water column in the adjacent estuary are critical in determining the water stratification in the Saguenay Fjord, since salinity and temperature control the density of waters that spill over the sill and fill the fjord's deep basins (Belzile et al., 2016). During most of the ice-free season, the St. Lawrence Estuary is characterized by three distinct layers: (1) a relatively warm and salty bottom layer (LSLE, 4°C < ~~T$_{max}$~~T < 6°C, 34 < S_P < 34.6; where T stands for temperature and S_P refers to practical salinity) that originates from mixing, on the continental shelf, of northwestern Atlantic and Labrador Current waters, (2) a cold intermediate layer (CIL, 30 - 150 m deep; -1°C < ~~T$_{max}$~~T < 2°C, 31.5 < S_P < 33) that forms in the Gulf of St. Lawrence in the winter and flows landward, and (3) a warm brackish surface layer (~~25–50~~0 - 30 m deep, -0.6°C < T < 12°C, 25 < S_P < 32) that results from the mixture of freshwater from various tributaries (mostly the St. Lawrence and Saguenay Rivers, but also north shore rivers such as the Betsiamites, Romaine and Manicouagan) and seawater and flows seaward to ultimately form the Gaspé Current (Dickie and Trites, 1983; El-Sabh and Silverberg, 1990; Gilbert and Pettigrew, 1997). Seasonal variations greatly affect the properties of the surface layer which merges with the intermediate layer during winter, as temperature and salinity change with atmospheric and buoyancy forcing and the contribution from tributaries decreases during winter months (Galbraith, 2006).

Likewise, the Saguenay Fjord is characterized by a strongly stratified water column that includes at least two water masses: (1) a warm, shallow layer, the Saguenay Shallow Water (SSW; 0°C < T < 16.8°C, 0.2 < S_P < 26.9), that lies above (2) the Saguenay Deep Water (SDW; 0.9°C < T < 4.0°C, 27.3 < S_P < 29.8). The SDW most likely forms from a mixture of surface fjord water, St. Lawrence River waters and the St. Lawrence Estuary Cold Intermediate Layer (CIL), when the latter spills over the entrance sill at the mouth of the fjord (Bourgault et al., 2012; Belzile et al., 2016). Nonetheless, our study shows that, because the Saguenay Fjord is a relatively deep fjord with multiple sills, the vertical structure of the water column is far more complex than described above.

2.2 Water-column sampling

The data presented in this paper were gathered on five cruises, between the years 2014 and 2018 aboard the R/V Coriolis II, in late spring (May 2016 and May 2018) and early summer (June 2017), as well as early and late fall (September 2014 and November 2017). Sampling of the water column was carried out with a rosette system along the central axis of the Saguenay Fjord, between St. Fulgence and the mouth of the fjord, including the Baie des Ha! Ha!. Stations in the St. Lawrence Estuary, near the mouth of the fjord, were also sampled. The sampling locations are identified in Fig. ~~(~~1.a~~)~~. The surface water of the Saguenay River was sampled, with a rope and bucket in 2013 and 2017, from the Dubuc Bridge that joins Chicoutimi and Chicoutimi-Nord, to determine the chemical characteristics of the freshwater Saguenay River end-member.

The rosette system (12 x 12-L Niskin bottles) was equipped with a Seabird 911Plus conductivity-temperature-depth (CTD) probe, a Seabird® SEB-43 oxygen probe, a WETLabs® C-Star transmissometer and a Seapoint® fluorometer. The Niskin bottles were closed at discrete depths as the rosette was raised from the bottom, typically at the surface (2-3 m), 25 m, 50 m, 75 m, 100 m, and at 50 m intervals to the bottom (or within 10 m of the bottom). Samples were taken directly from the bottles for dissolved oxygen (DO), ~~pH$_{(NBS)}$~~pH_{NBS} and/or ~~pH$_{(total)}$~~pH_T,

total alkalinity (TA), dissolved inorganic carbon (DIC), dissolved silicate (DSi), practical salinity (S_P), and the stable oxygen isotopic composition of the water ($\delta^{18}O_{water}$). Water samples destined for pH measurements were transferred to 125 mL plastic bottles without headspace whereas TA and TA/DIC samples were stored in, respectively, 250 mL and 500 mL glass bottles. TA and TA/DIC samples were poisoned with a few crystals of mercuric chloride ($HgCl_2$) and bottles were sealed using a ground-glass stopper and Apiezon® Type-M high-vacuum grease. $\delta^{18}O_{water}$ and S_P samples were stored in 13 mL plastic screw-cap test tubes.

Direct measurements of surface water (~ 2 m) pCO_2 were carried out using a CO_2-Pro CV (Pro-Oceanus, Bridgewater, NS) probe in May 2018. The CO_2-Pro CV probe operates through rapid diffusion of gases through a supported semi-permeable membrane to a thermostated cell in which the CO_2 mole fraction is quantified by a non-dispersive infrared detector (NDIR) that was factory calibrated using standard trace gas mixtures. The instrument was operated in continuous mode, with measurements taken nearly every 7 seconds. Stable pCO_2 values were achieved after a 15-minute equilibration period and averaged over the next 20 minutes. Relative standard deviations over this period were typically on the order of 0.2 to 6% but were on the order of 0.1% in a stable water mass at 220 m depth, implying that deviations recorded at the surface likely reflected natural variations over the period of sampling as the ship drifted with the current. The manufacturer claims a 1% accuracy, but the performance of the instrument may be even better (Hunt et al., 2017).

Total freshwater discharge data of the Saguenay River were provided by Rio Tinto Alcan (a multinational aluminium smelter/producer that manages its own hydroelectric dam on the Saguenay River) from their bank stabilization programme. Data for the relevant sampling days in September 2014, May 2016, June 2017, November 2017 and May 2018 were taken from the Shipshaw and Chute-à-Caron monitoring stations.

2.3 Analytical procedures

T and S_P were determined in-situ using the CTD probe. The conductivity probe was calibrated by the manufacturer over the winter prior to the cruises. In addition, the S_P of surface waters was determined by potentiometric argentometric titration at McGill University and calibration of the $AgNO_3$ titrant with IAPSO standard seawater. The reproducibility of these measurements is typically better than ± 0.5%.

pH_T was determined spectrophotometrically on board, on the total hydrogen ion concentration scale for saline waters (S_P > 5), using phenol red and purified m-cresol purple as indicators and a Hewlett-Packard UV-visible diode array spectrophotometer (HP-8453A) with a 5-cm quartz cell, after thermal equilibration of the sample in a constant temperature bath at 25°C ± 0.1. The salinity-dependence of the dissociation constants and molar absorptivities of the indicators were taken from Robert-Baldo et al. (1985) for phenol red and from Clayton and Byrne (1993) for m-cresol purple. The salinity-dependence of the phenol red indicator dissociation constant and molar absorptivities was extended (from S_P = 5 to 35; Bellis, 2002) to encompass the range of salinities encountered in this study, but computed pH_T values from the revised fit were not significantly different from those obtained with the relationship provided by Robert-Baldo et al. (1985). Results computed from these parameters yielded results that were more similar to each other as well as to potentiometric glass electrode measurements than the revised equation for the purified m-cresol purple provided by Douglas and Byrne (2017). The pH of low-salinity waters (S_P < 5) was determined

potentiometrically on board at 25°C, on the NIST (formerly NBS) scale (~~pH_{NIST}~~pH_{NBS}), using a Radiometer Analytical® (GK2401C) combination glass electrode connected to a Radiometer Analytical® pH/millivoltmeter (PHM84). A calibration of the electrode was completed prior to and after each measurement, using three NIST-traceable buffer solutions: pH-4.00, pH-7.00 and pH-10.00, at 25°C. The Nernstian slope was then obtained from the least-squares fit of the electrode response to the NIST buffer values. For waters with S_P comprised between 5 and 35, pH_{NBS} was converted to pH_T according to the electrode response to TRIS buffer solutions prepared at S_P = 5, 15, 25 and 35 and for which the pH_T was assigned at 25°C (Millero, 1986). Reproducibility of pH measurements based on replicate analyses of the same sample or at least two of the three methods used was typically better than ± 0.005.

Dissolved oxygen (DO) concentrations were determined on board by Winkler titration on distinct water samples recovered directly from the Niskin bottles, following the method described by Grasshoff et al. (1999). The relative standard deviation, based on replicate analyses of samples recovered from the same Niskin bottle, was 0.5 %. These measurements served to calibrate the SBE-43 oxygen probe mounted on the rosette sampler.

The stable oxygen isotopic composition of the water samples ($\delta^{18}O_{water}$) was determined using the CO_2 equilibration method of Epstein and Mayeda (1953). Aliquots (200 µL) of the water samples and three laboratory internal reference waters were transferred into 3 mL vials stoppered with a septum cap. The vials were then placed in a heated rack maintained at 40°C. Commercially available 99.998% pure CO_2 gas (Research Grade) was introduced in all the vials using a Micromass AquaPrep and allowed to equilibrate for 7 hours. The headspace CO_2 was then sampled by the Micromass AquaPrep, dried on a -80°C water trap, and analyzed on a Micromass Isoprime universal triple collector isotope ratio mass spectrometer in dual inlet mode at the GEOTOP-UQAM Stable Isotope Laboratory. Data were normalized against the three internal reference waters, themselves calibrated against Vienna Standard Mean Ocean Water (V-SMOW) and Vienna Standard Light Arctic Precipitation (V-SLAP). The results are reported on the δ-scale in ‰ relative to V-SMOW:

$$\delta^{18}O = \left(\frac{(^{18}O/^{16}O)_{sample}}{(^{18}O/^{16}O)_{standard}} - 1\right) \times 1000 \quad (1)$$

Based on replicate analyses of the samples, the average standard deviation of the measurements was better than 0.05‰.

TA was measured using an automated Radiometer (TitraLab865®) potentiometric titrator and a Red Rod® combination pH electrode (pHC2001) at McGill University. The dilute HCl titrant was calibrated prior, during and after each titration session using certified reference materials (CRM) provided by Andrew Dickson (Scripps Institution of Oceanography). Raw titration data were processed with a proprietary algorithm designed for shallow end-point detection. Surface water samples from the Saguenay Fjord and the Upper St. Lawrence Estuary were also analyzed at Dalhousie University using a VINDTA 3C® (Versatile Instrument for the Determination of Titration Alkalinity, by Marianda) following the method described in Dickson et al. (2007). A calibration of the instrument was performed against CRMs and the reproducibility of the measurements was better than 0.1%.

The DIC concentration of samples, recovered in 2016, 2017 and 2018 in the Saguenay Fjord and surface waters of the Upper and Lower St-Lawrence Estuary, were determined at Dalhousie University using the VINDTA

3C®. In 2014, DIC was determined on board using a SciTech Apollo DIC analyzer. Once thermally equilibrated at 25°C, 1-1.5 mL of the sample was acidified with 10% H_3PO_4 after being injected into the instrument's reactor. The evolved CO_2 was carried to a LI-COR infrared analyzer by a stream of pure nitrogen. A calibration curve was constructed using gravimetrically prepared Na_2CO_3 solutions, and the accuracy of the measurements was verified using a CRM. Reproducibility was typically on the order of 0.2%.

2.4 Calculations

2.4.1 Water mass distribution analysis

A combination of transport processes associated with ocean circulation and biogeochemical cycles generally controls the distribution of tracers in the ocean (Chester, 1990). Resolving the effects of mixing and biogeochemical cycling is imperative if one is to evaluate the movement of nutrients and tracers in a water body. An Optimum Multi-Parameter (OMP) analysis allows for the determination of the relative contributions of pre-defined source-water types (SWT), representing the parameter values of the unmixed water masses in one specific geographic location, by optimizing the hydrographic data gathered in a given system (Tomczak, 1981). The original OMP algorithm is a linear inverse model that assumes all hydrographic tracers are conservative. The algorithm has since been modified to handle non-conservative properties such as DIC and nutrients by taking into consideration the stoichiometry of microbial respiration and photosynthesis (Dinauer and Mucci, 2018; Karstensen and Tomczak, 1998).

OMP calculates the SWT fractions, x_i, for each data point by finding the best linear mixing combination defined by parameters such as T, S_P, $\delta^{18}O_{water}$, DO, TA, and DIC. The contributions from all SWT must add-up to 100% and cannot be negative. Assuming that four SWT (a, b, c, and d) are sufficient to characterize the water column structure, and six parameters (T, S, $\delta^{18}O_{water}$, DO, TA, and DIC) characterize each of these, the following set of linear equations is solved in the classical OMP analysis (MATLAB - version 1.2.0.0; Karstensen, 2013):

$$x_a T_a + x_b T_b + x_c T_c + x_d T_d = T_{obs} + R_T \quad (2.a)$$

$$x_a S_a + x_b S_b + x_c S_c + x_d S_d = S_{obs} + R_S \quad (2.b)$$

$$x_a \delta^{18}O_a + x_b \delta^{18}O_b + x_c \delta^{18}O_c + x_d \delta^{18}O_d = \delta^{18}O_{obs} + R_{\delta^{18}O} \quad (2.c)$$

$$x_a DO_a + x_b DO_b + x_c DO_c + x_d DO_d = DO_{obs} + R_{DO} \quad (2.d)$$

$$x_a TA_a + x_b TA_b + x_c TA_c + x_d TA_d = TA_{obs} + R_{TA} \quad (2.e)$$

$$x_a DIC_a + x_b DIC_b + x_c DIC_c + x_d DIC_d = DIC_{obs} + R_{DIC} \quad (2.f)$$

$$x_a + x_b + x_c + x_d = 1 + R_{\sum} \quad (2.g)$$

where T_{obs}, S_{obs}, $\delta^{18}O_{obs}$, DO_{obs}, TA_{obs}, and DIC_{obs} are the observed values in any given parcel of water and ~~$R_{\bar{s}}$~~R are their respective associated fitting residuals. T_i, S_i, $\delta^{18}O_i$, DO_i, TA_i, and DIC_i (i= a, …, d) are the characteristic values of each SWT (Lansard et al., 2012; Tomczak and Large, 1989; Mackas et al., 1987). Mass conservation is expressed in Eq. (2.g).

Formatted: Font: Not Bold

To account for potential environmental variability, measurement inaccuracies, and allow for the comparison of parameters with incommensurable units, a weighting procedure based on covariances between tracers is applied. In this study, weights were assigned arbitrarily based on their conservative behaviors and variability (Lansard et al., 2012). Conservative tracers (i.e. S_P, TA, $\delta^{18}O_{water}$) were ~~appointed~~assigned heavy weights, while non-conservative tracers (i.e. T, DO, DIC) were given low weights according to their seasonal variability. For instance, temperatures in the surface waters of the Saguenay River range from 3.1°C in the winter to 21°C in the summer. Dissolved oxygen was also considered a non-conservative tracer as it is heavily reliant on temperature and salinity, as well as biological activity. DIC was given an intermediate weight given that it is relatively conservative except in the surface waters, where photosynthesis and air-sea gas exchange take place. Several OMP analyses were carried out using different weights for each parameter, while weighing their conservative behaviour appropriately (i.e., highly conservative vs. lightly conservative). Results were not affected significantly.

2.4.2 Source-Water Type definitions

A water mass is, by definition, a body of water having its origin in a particular source region (Tomczak, 1999). An OMP analysis requires the user to define the major water masses contributing to the structure of the water column in the study area. In the context of biogeochemical cycles, a SWT should be defined where the water mass enters the basin, ~~upstream from~~before it enters the mixing region (Karstensen, 2013). Parameter values are preferably extrapolated from hydrographic observations in the water mass formation region or can be found in the literature.

In this study, source-water type definitions were derived from property-property diagrams (See Appendix, Fig. A) of an observational dataset relevant to the Saguenay Fjord: the Saguenay River (SWR), the St. Lawrence Estuary summertime Cold Intermediate Layer (CIL), the Lower St. Lawrence Estuary bottom waters (LSLE) and the St. Lawrence River (SLRW). Each definition was captured relative to the fjord, i.e. each source-water type is only appropriate for the fjord and for the period of study. Definitions and weights are reported in Table 1. A seasonality analysis was carried out to ensure SWT definitions were appropriate for the period of study. Insignificant variations were observed in tracers such as $\delta^{18}O$, DIC, TA, DO and S_P. The only highly variable tracer was T, which was given the lowest possible weight in the OMP analysis.

2.4.3 CO_2 partial pressures

The CO_2 partial pressure in seawater ($pCO_{2(SW)}$) is defined as the pCO_2 in water-saturated air ($pCO_{2(air)}$) in equilibrium with the water sample or the ratio of the CO_2 concentration in solution to the equilibrium concentration at T, P and S_P, multiplied by the actual $pCO_{2(air)}$. As direct measurements of the surface mixed layer pCO_2 were not available in September 2014, May 2016, June 2017 and November 2017, it was calculated ($pCO_{2(SW-calc)}$) using CO2SYS (Excel v2.1; Pierrot et al., 2006) and the measured pH (total or NBS/NIST scale; see Appendix, Fig. B.1 and B.2), DIC ($\mu mol \cdot kg^{-1}$), in-situ temperature (°C), practical salinity (S_P) and pressure (dbar) as input parameters. When available, soluble reactive phosphate (SRP) and dissolved silicate (DSi) concentrations were also included in the calculations, but their inclusion did not affect the results significantly because their concentrations are relatively low in surface waters (0.49 µM and 37.0 µM, respectively) and introduce an insignificant error. DIC rather than TA

Formatted: English (United Kingdom)

Formatted: English (United Kingdom)

Formatted: English (United States)

was used as an input parameter to CO2SYS since the fjord surface waters are enriched in colored dissolved organic carbon (> 4 mg/L) delivered by the Saguenay River, and are characterized by a negative organic alkalinity (positive organic acidity) (see below). The carbonic acid dissociation constants (K^*_1 and K^*_2) of Cai and Wang (1998) were used for the calculations, as the latter were found to be more suitable for the low-salinity ~~conditions~~waters encountered in estuarine environments such as the Saguenay Fjord ($S_P < 20$) (Dinauer and Mucci, 2017). $pCO_{2(SW\text{-}calc)}$ values were computed for the surface mixed layer located above the sharp pycnocline (~10 m) where most physical and chemical properties are directly impacted by biological activity (photosynthesis and respiration) as well as heat and gas exchange across the air-sea interface (Table 2). Direct measurements of pCO_2 ($pCO_{2(SW\text{-}meas)}$) were acquired in May 2018, and $pCO_{2(SW\text{-}calc)}$ were also calculated from pH and DIC for this sampling month for comparison purposes, following the aforementioned procedure.

2.4.4 CO_2 flux across the air-sea interface

The difference between the air and sea-surface pCO_2 values ($\Delta pCO_2 = pCO_{2(SW)} - pCO_{2(air)}$) determines the direction of gas exchange and whether the surface mixed layer of a body of water is a source or a sink of CO_2 for the atmosphere. The air-sea CO_2 gas exchange, or CO_2 flux, can be estimated at each station using the following relationship:

$$FCO_2 = k \cdot K_0 \cdot (\Delta pCO_2) \quad (3.a)$$

where F is the flux of CO_2 across the air-sea interface in mmol·m^{-2}·d^{-1}, k is the gas transfer velocity of CO_2 in cm·h^{-1} (Wanninkhof, 1992), K_0 is the solubility of CO_2 in mol·kg^{-1}·atm^{-1} at the in-situ temperature and salinity of the surface waters (Weiss, 1974), and ΔpCO_2 is the difference between the air and sea-surface pCO_2 values in µatm. Whereas, formally, Fick's first law of diffusion should be written as $F = -D$ ~~$\delta c/\delta x$, as commonly expressed by Eq.~~$\delta C/\delta x$ (where F is the diffusion flux in mole sec^{-1} m^{-2}, D is the diffusion coefficient in m^2 sec^{-1}, C is the concentration of CO_2 in mole m^{-3} and x is the distance in m), as commonly expressed by Eq. (3.a), positive values of F indicate the release of CO_2 to the atmosphere by surface waters, whereas negative values imply that surface waters serve as a sink of atmospheric CO_2. The flux of CO_2 was computed for each sampling month, using the $pCO_{2(air)}$ for each sampling date (395 µatm for September 2014, ~~and~~ 407 µatm for May 2016, 408 µatm for June and November 2017, and 411 µatm for May 2018 – see below for details).

The gas transfer velocity of CO_2 was calculated using the revised relationship of Wanninkhof (2014):

$$k = 0.215u^2\,(Sc/660)^{-1/2} \quad (3.b)$$

where u is the wind speed (m s^{-1}) and Sc is the Schmidt number (Wanninkhof, 2014). Wind speed was estimated using the hourly station wind speed data from Environment Canada at the La Baie weather station~~,~~ (Fig. 1.a), for each sampling month. The Schmidt number is defined as the kinematic viscosity of water divided by the diffusion coefficient of CO_2. Sc was corrected for the temperature dependence of CO_2 in freshwater ($S_P = 0$), assuming that k

is proportional to $Sc^{-1/2}$ (Wanninkhof, 1992). In the case of CO_2, the increase in $Sc^{-1/2}$ (and k) with increasing temperature is compensated for by a decrease in solubility, therefore k was considered nearly temperature independent (Wanninkhof, 1992). Sc was computed using:

$$Sc = A + Bt + Ct^2 + Dt^3 + Et^4 \quad (3.c)$$

where t is the temperature (degrees Celcius) and A, B, C, D and E are fitting coefficients for seawater (S_P = 35) and freshwater (S_P = 0), for water temperatures ranging from -2°C to 40°C (Wanninkhof, 2014). The uncertainty in Sc ranges from 3 to 10% and is mainly due to the imprecision of diffusion coefficients (Wanninkhof, 2014). Estimates of k, calculated at each sampling point using the equation of Wanninkhof (2014), ranged from 0.36 to 3.38 cm·h^{-1} for the fjord, compared to 1.6 to 4.5 cm·h^{-1} in the St. Lawrence Estuary (Dinauer and Mucci, 2017).

Atmospheric pCO_2 values ($pCO_{2(air)}$) were computed using the daily averages of measured mole fractions of CO_2 in dry air, obtained at the La Baie weather station and retrieved from the Climate Research Division at Environment and Climate Change Canada. The mean $pCO_{2(air)}$ was then calculated for each year using the following equation:

$$pCO_{2(air)} = xCO_2 \cdot (P_b - P_w) \quad (4)$$

where xCO_2 is the measured mole fraction of CO_2 in dry air in ppm, P_b is the barometric pressure at the sea surface in atm, and P_w is the saturation water vapor pressure at in-situ temperature and salinity, in atm. P_b was obtained using the conversion formula of Tim Brice and Todd Hall (from NOAA's National Weather Service - https://www.weather.gov/epz/wxcalc_wxcalc2go), using the La Baie weather station's elevation (152 m). P_w was calculated using the Rivière-à-Mars properties (i.e. closest body of water to the weather station) and the P_w calculated from its relationship to T and S_P provided by Weiss and Price (1980).

The area-averaged CO_2 flux ($F_{area\text{-}avg}$) was computed for the whole fjord, following the procedure described by Jiang et al. (2008):

$$F_{area-avg} = \frac{\Sigma F_i \times S_i}{\Sigma S_i} \quad (5)$$

where F_i is the average of all the fluxes within segment i, and S_i is the surface area of segment i. The fjord was divided into two segments, one including the inner basin and the other encompassing the two outer basins, as each segment often displays distinct behaviors. Segments are identified in Fig. 1.b. The fjord's surface area (~290 km^2) was computed using a land mask in MATLAB.

2.4.5 Water Mixing Model

A two end-member mixing model was constructed based on the chemical properties of the freshwater delivered to the fjord (Saguenay River) and marine bottom waters entering the fjord from the St. Lawrence Estuary (Fig. 2 .a).

As shown in the results of the OMP analysis (Sect. 3.1), the LSLE and SLRW have a negligible influence on the fjord's water structure, and thus were not included in the model. Given that the carbonate chemistries of the CIL and LSLE waters are similar, the bottom waters were assumed to be well mixed and constitute a single end-member. This is illustrated in Fig. (2), as the high S_P end-member alkalinity extends linearly beyond that of the CIL end-member (Table 1). The measured surface TAs were strongly correlated to S_P ($R^2 = 0.99$) in the fjord waters. Therefore, end-member properties were obtained by extrapolating the surface water (above the pycnocline) data to $S_P = 0$ and bottom-water data to the highest measured salinity (Fig. 2.a). The extrapolated $TA_{(meas)}$ (Fig 2.b; 154 µmol·kg^{-1}) is in good agreement with the average $TA_{(meas)}$ of samples taken directly from the Saguenay River in 2013 and 2017 (157 µmol·kg^{-1}). The organic alkalinity of the fjord waters was estimated from the difference between the measured and calculated TA ($TA_{(calc)}$; Fig. 2.b). The latter was calculated using CO2SYS (Excel v2.1; Pierrot et al., 2006) and pH and DIC as input parameters. The end-member source waters were then mixed, assuming that $TA_{(calc)}$ and DIC behave conservatively. Hence, the salinity, total alkalinity ($TA_{(mix)}$) and dissolved inorganic carbon ($DIC_{(mix)}$) of the mixed solutions were calculated using the following equations:

$$S_{P(mix)} = \frac{m_1 S_{P1} + m_2 S_{P2}}{(m_1 + m_2)} \quad (6a)$$

$$TA_{(mix)} = \frac{m_1 TA_{(calc)-1} + m_2 TA_{(calc)-2}}{(m_1 + m_2)} \quad (6b)$$

$$DIC_{(mix)} = \frac{m_1 DIC_1 + m_2 DIC_2}{(m_1 + m_2)} \quad (6c)$$

where ~~mi~~m_i are the mass contributions of each end-member to the mixture.

$pCO_{2(SW\text{-}mix)}$ was then computed from $TA_{(mix)}$ and $DIC_{(mix)}$ for practical salinities ranging from 0 to 33, at four different temperatures (0°C, 5°C, 10°C and 15°C) using CO2SYS. Results of the model (Fig. 8) show that, at the lower and higher salinities, the $pCO_{2(SW\text{-}mix)}$ is elevated, and the fjord serves as a net source of CO_2 to the atmosphere, but at intermediate salinities ($5 < S_P < 15$) or mixing ratios, the fjord may serve as a net sink of atmospheric CO_2 when surface water temperatures are close to freezing. The data from the various cruises are superimposed on the model results, after correction for the organic alkalinity.

2.4.6 Salinity normalization of DIC in surface waters

To quantitatively evaluate the impact of biological activity on the DIC budget in the surface waters of the fjord, DIC and $TA_{(calc)}$ were normalized to the average surface salinity of each sampling month (S_P = 12.4 for September 2014, S_P = 2.58 for May 2016, S_P = 7.61 for June 2017, S_P = 10.9 for November 2017 and S_P = 5.9 for May 2018) following the procedure of Friis et al. (2003):

$$\mathrm{NDIC} = \frac{DIC^{meas} - DIC^{S=0}}{S^{meas}} \cdot S^{ref} + DIC^{S=0} \quad (7)$$

where DIC^{meas} is the measured DIC, $DIC^{S=0}$ is the DIC extrapolated to $S_P = 0$, S^{meas} is the measured practical salinity and S^{ref} is the average measured practical salinity per sampling month (Friis et al., 2003). The change in

NDIC (i.e. ΔNDIC) along the fjord, relative to the waters at the head of the fjord, was then computed for each sampling month. These values reveal how DIC evolves along the fjord beyond what is expected based on conservative mixing.

2.4.7 Oxygen saturation and apparent oxygen utilization in the surface waters

To further account for the biological activity in the surface waters, the oxygen saturation index was calculated for each sampling month in the surface waters of the fjord using:

$$\%\, sat = ([O_2]_{meas}/[O_2]_{equil}) \times 100 \quad (8)$$

where $[O_2]_{meas}$ is the dissolved oxygen concentration measured in the fjord waters, and $[O_2]_{equil}$ is the equilibrium dissolved oxygen concentration (or solubility) at in-situ conditions (i.e. temperature and salinity) for each sample.

The oxygen saturation index indicates if the system is autotrophic (i.e. production of oxygen, dominated by photosynthesis) or heterotrophic (consumption of oxygen, dominated by microbial respiration). The oxygen saturation remains a qualitative proxy as O_2 exchange at the air-sea interface is about 9 times faster than CO_2 exchange (Zeebe and Wolf-Gladrow, 2001). The apparent oxygen utilization (AOU) was also computed from the difference between $[O_2]_{equil}$ and $[O_2]_{meas}$.

3 Results and discussion

3.1 Water mass analysis

Relative contributions (mixing ratios, f) of the Saguenay River (SRW), the St. Lawrence Estuary summertime Cold Intermediate Layer (CIL) ~~from the St. Lawrence Estuary~~ and Lower St. Lawrence Estuary (LSLE) bottom waters throughout the Saguenay Fjord's water column for the sampling month of June 2017 are shown in Fig. (3). As expected, the SRW and CIL are dominant contributors, with the SRW forming a brackish surface layer (f = 1 in surface waters), and the CIL replenishing the bottom waters of the fjord ($0.7 < f < 1$). According to the OMP analysis, the LSLE bottom waters have a small contribution to the fjord's bottom waters (f = 0.2), adding to the complexity of the water structure. Although somewhat unexpected, this can readily be explained by tidal upwelling, internal waves and intense turbulent mixing of the water column resulting from the rapid shoaling at the head of the Laurentian Channel (Gratton et al., 1988; Saucier and Chassé, 2000). The relative contribution of the LSLE bottom waters in the deep waters of the fjord is small and could only be detected because of the suite of geochemical and isotopic tracers used in the OMP analysis, especially the difference in the $\delta^{18}O_{water}$ signature of the CIL and LSLE waters. The contribution from the St. Lawrence River Water (SLRW) is negligible, as it intrudes slightly at the surface at the mouth of the fjord and is thus not shown here. Although the water column structure is similar throughout the year, seasonal variations do occur and will be addressed in a forthcoming paper.

Formatted: Indent: First line: 0 cm

3.2 Aqueous pCO_2 and CO_2 flux

Variations of the inorganic carbon chemistry in the Saguenay Fjord water column are described using field data acquired in September 2014, May 2016, June 2017, November 2017 and May 2018. ~~The river drains the Canadian Shield and boreal forest soils, and carries organic acidity released from soil porewaters.~~ The organic alkalinity (acidity) accounted, on average, for 2.2% to 11.9% of the total alkalinity of the Saguenay River and varied annually and seasonally (-21 $\mu mol \cdot kg^{-1}$ in September 2014, -39 $\mu mol \cdot kg^{-1}$ in May 2016, -49 $\mu mol \cdot kg^{-1}$ in June 2017, -22 $\mu mol \cdot kg^{-1}$ in November 2017 and -18 $\mu mol \cdot kg^{-1}$ in May 2018). It was inversely proportional to the salinity of the surface waters of the fjord and became positive ~~but~~yet a negligible fraction (< 0.1%) of $TA_{(corr)}$ at $S_P > 25$, like in the St. Lawrence Estuary. The negative organic alkalinity of the Saguenay River water most likely originates from soil humic acids that are flushed by percolation with groundwaters that drain the metamorphic and igneous rocks of the Canadian Shield. Surface-water pCO_2 ($pCO_{2(SW-calc)}$) values were higher at the head of the fjord (i.e. near the Saguenay River mouth) and lower at the mouth of the fjord, although large variations (315 µatm to 740 µatm – average 503 µatm) were observed on a seasonal and yearly basis (Table 2). Values of $pCO_{2(SW)}$ were higher in May 2018 (623 µatm), June 2017 (506 µatm) and May 2016 (563 µatm) than in November 2017 (418 µatm) and September 2014 (406 µatm). This can be explained by the larger freshwater discharge from the Saguenay River in the spring (i.e. spring freshet, average of 1856 ± 21 $m^3 s^{-1}$ for spring periods of 1998 - 2018), compared to the fall (1470 ± 10 $m^3 s^{-1}$ for fall periods of 1998 - 2018). As atmospheric $pCO_{2(air)}$ varied marginally between September 2014 (395 µatm) and May 2018 (411 µatm), the fjord was generally a source of CO_2 to the atmosphere near its head (i.e. surface pCO_2 values above atmospheric level), while the zone near its mouth was most often a sink (i.e. surface pCO_2 values below atmospheric level) (Fig. 4). An anomaly was observed in November 2017, with a high $pCO_{2(SW-calc)}$ value (> 550 µatm) near the mouth of the fjord. Given the statistics of the box plot presented in Fig. (7), this value appears to be erroneous.

Air-sea CO_2 fluxes within the fjord ranged from -2.4 $mmol \cdot m^{-2} \cdot d^{-1}$ to 10.0 $mmol \cdot m^{-2} \cdot d^{-1}$ (Fig. 6). Near the head of the fjord, fluxes were mostly positive, while values decreased when approaching its mouth. Overall, the total area-averaged degassing flux of the fjord adds up to 2.14 ± 0.43 $mmol \cdot m^{-2} \cdot d^{-1}$ ~~(i.e.~~or 0.78 ± 0.16 $mol \cdot m^{-2} \cdot yr^{-1}$~~).~~. In comparison, the degassing flux in the adjacent St. Lawrence Estuary was estimated at between 0.36 and 0.74 $mol \cdot m^{-2} \cdot yr^{-1}$ during the late spring and early summer (Dinauer and Mucci, 2017). This discrepancy can be explained by the low carbonate alkalinity (and buffer capacity) of the Saguenay River waters that flow through the Grenvillian metamorphic and igneous rocks of the Canadian Shield (Piper et al., 1990), as with most rivers on the north shore of the St. Lawrence Estuary (e.g., Betsiamites, Manicouagan, Romaine; Paul del Giorgio, pers. comm.), and the low productivity of the fjord surface waters because of very limited light penetration due to their high chromotrophic dissolved organic matter (CDOM) content (Tremblay and Gagné, 2009; Xie et al., 2012). In contrast, waters of the St. Lawrence River have an elevated carbonate alkalinity (~1200 µM), inherited from the Ottawa River that drains through limestone deposits (Telmer and Veizer, 1999). Furthermore, the Estuary is host to multiple seasonal phytoplankton blooms (Levasseur and Therriault, 1987; Zakardjian et al., 2000; Annane et al., 2015) that strongly modulate its trophic status (Dinauer and Mucci, 2018).

The correlation between $pCO_{2(SW-meas)}$ and $pCO_{2(SW-calc)}$ is presented in Fig. (5). The average difference between $pCO_{2(SW-meas)}$ and $pCO_{2(SW-calc)}$ is 48 µatm, implying that calculations underestimate $pCO_{2(SW)}$ values by approximately

Formatted: Font: Bold, English (United Kingdom)

7% and thus contribute to the uncertainty associated with CO_2 fluxes. This discrepancy most likely originates from uncertainties associated with the carbonic acid dissociation constants (K^*_1 and K^*_2) in low salinity estuarine environments, particularly those affected by strong organic alkalinities or acidities such as in the Saguenay Fjord (Cai et al., 1998; Ko et al., 2016). This concurs with the results ~~from~~of Lueker et al. (2000) who showed that, depending on the choice of K^*_1 and K^*_2, computed $pCO_{2(SW)}$ values from other carbonate system parameters (TA, DIC, pH) can be up to 10% lower than those of direct measurements. Consequently, although the constants of Cai and Wang (1998) are the most suitable for this study, direct measurements of the $pCO_{2(SW)}$ should preferentially be carried out whenever possible.

3.3 Water Mixing Model approach

As results of the OMP analysis reveal, LSLE and SLRW have a negligible influence on the water properties in the fjord, except for the latter near the mouth. Additionally, given the relatively small contribution of the LSLE deep waters and their similarity to the carbonate chemistry of the CIL, their influence is considered inconsequential on the properties of the mixture. Hence, a conservative mixing model was constructed based on the chemical properties of the two main source ~~–~~water masses in the fjord (i.e.~~.~~, SRW and the CIL mixture for bottom waters), and the relationship between practical salinity and $TA_{(corr)}$/DIC, respectively (Fig. 8). $pCO_{2(SW-calc)}$ were normalized at each station to the average surface water temperature per sampling month (i.e., T = 10.4°C for September 2014, T = 5.04°C for May 2016, T = 11.9°C for June 2017, T = 7.13°C for November 2017 and T = 5.08°C for May 2018) to account for the effects of temperature on the CO_2 solubility in water, following the procedure described in Jiang et al. (2008). The temperature-normalized $pCO_{2(SW-calc)}$ values, $pCO_{2(SW-SST)}$, from the various cruises were superimposed on the model results in Fig. (8).

Field measurements follow the trend displayed by the mixing model. The fjord appears to be a net source of CO_2 to the atmosphere during periods of high freshwater discharge (i.e. spring freshet) and a net sink at intermediate surface salinities ($5 < S_P < 15$). This is consistent with the weak buffer capacity of the freshwater. Given the short residence time of surface waters in the Saguenay Fjord (~ 1.5 days), the influence of gas exchange across the air-sea interface is negligible on the DIC pool. Likewise, Dinauer and Mucci (2017) reported that the surface waters in the St. Lawrence Estuary near Tadoussac (at the mouth of the fjord) are highly supersaturated in CO_2 with respect to the atmosphere and only the highly productive waters of the Lower Estuary manage to draw down the surface pCO_2 to near atmospheric values. In other words, degassing of the metabolic CO_2 accumulated in the river and upper estuary is slow. Thus, changes in temperature-normalized pCO_2 primarily ~~mostly~~ reflect changes in DIC by mixing and biological activity. Hence, discrepancies between results of the mixing model and field measurements can be ascribed to microbial respiration and photosynthesis.

In May 2016, the surface waters of the fjord were clearly supersaturated in oxygen (Fig. 9), implying that photosynthesis dominated over respiration. This would explain the rapid seaward (increasing S_P) decrease in $pCO_{2(SW-SST)}$, faster than the mixing model predicts (Fig. 8), and the strong negative ΔNDIC (i.e. change in NDIC relative to the saline waters at the head of the fjord) throughout the fjord (Fig. 10), as CO_2 (i.e. DIC) is taken up by photosynthesizing organisms - most likely diatoms (Chassé and Côté, 1991). In May 2018, surface waters were slightly

Formatted: Subscript

undersaturated in oxygen, between 90% and 100% saturation, and ΔNDIC was positive over most of the fjord. Very similar trends were observed in June 2017, with near-saturation oxygen concentrations (between 95 and 101% saturation) and mostly positive ΔNDIC values throughout the transect. Thus, during these sampling periods, biological activity was dominated by microbial respiration (Fig. 10), elucidating the minor deviation between the $pCO_{2(SW-SST)}$ and the model results (Fig. 8), especially near the head of the fjord. Additionally, it is interesting to note that ΔNDIC is chronically negative for all sampling months near the 45 km mark.

The difference between the May 2016 and May 2018 biological responses to the spring freshet can potentially be explained by the difference in total freshwater discharge from the Saguenay River to the fjord. The freshwater discharge in May 2018 was approximately 20% larger than in May 2016. Whereas the surface salinities recorded both years throughout most of the fjord were nearly identical (S_P = 0.5-4 in 2016, S_P= 0.7-5 in 2018), the greater delivery of soil porewater and associated CDOM in May 2018 may have inhibited local productivity due to light absorption by CDOM (Lavoie et al., 2007). Consistent with this interpretation is the fact that the $pCO_{2(SW-SST)}$ at the head of the fjord (St. Fulgence) in May 2016 was slightly higher than in May 2018 but was drawn down much faster downstream (Fig. 8).

There does not appear to be a clear biological signal in the November 2017 data, as little variation is observed between the measured and modeled pCO_2. Furthermore, Fig. (10) indicates that neither respiration nor photosynthesis dominated during this period as the ΔNDIC varies between weakly positive and negative values. Likewise, the September 2014 data reveal little biological activity, although a slight dominance of respiration (i.e. positive ΔNDIC with a drop in $\%O_2$ saturation) can be observed near the mouth of the fjord (Fig. 10), hence explaining the slight deviation from the mixing model.

These results highlight the importance of the freshwater plume from the Saguenay River in regulating the pCO_2 dynamics in the fjord. Winds, in addition to regulating the gas exchange coefficient, are also known to have a direct influence on air-sea CO_2 fluxes by driving upwelling of CO_2-rich waters along with the entrainment of nutrients in surface waters, thus increasing biological activity (Wanninkhof and Triñanes, 2017). However, wind speeds are relatively low in the studied system (1.89 m s^{-1} < u < 4.2 m s^{-1}, Table 2), implying a calm sea state (Frankignoulle, 1998), and hence reinforcing that changes in $pCO_{2(SW-SST)}$ can mainly be attributed to microbial respiration and photosynthesis modulated by water renewals rather than winds.

4 Summary and conclusions

Results of the OMP analysis reveal that SRW and CIL are the dominant source-water types to the fjord and determine the structure of its water column. Mixing of marine waters with SRW at the head of the fjord leads to the formation of a brackish surface layer (wedge) while the CIL replenishes the bottom waters of the fjord. The analysis further unveiled a small contribution of the LSLE bottom water to the bottom waters of the fjord, adding to the complexity of the water column structure. The SLRW has a negligible influence on the water properties in the fjord, except near its mouth - sampling of the very turbulent waters directly over the fjord's first and shallowest sill would help refine the contribution of the SLRW to the fjord's surface waters.

The magnitude and sign of the ΔpCO_2 across the air-water interface in the Saguenay Fjord, mostly determined by the $pCO_{2(SW)}$ as $pCO_{2(air)}$ ~~varying~~varied only slightly over the sampling period, are mostly modulated by the freshwater discharge and the salinity of the surface waters. The surface waters of the fjord are a source of CO_2 to the atmosphere at high freshwater discharge, and a sink of CO_2 at intermediate surface salinities ($5 < S_P < 15$), especially at near-freezing temperatures. Direct measurements of surface-water pCO_2 acquired in May 2018 ~~further validate~~confirmed this trend. ~~–~~Biological activity ~~(photosynthesis and respiration)~~ alters the surface-water pCO_2, with both photosynthesis and respiration impacting the waters depending on the sampling month. ~~-~~This conclusion is ~~further~~ supported by the oxygen saturations observed in the surface waters of the fjord, as well as the downstream ΔNDIC trend along the fjord's main axis. Given the short residence time of surface waters in the Saguenay Fjord (~ 1.5 days), the influence of gas exchange on spatial variations of the ΔpCO_2 across the air-sea interface along the main axis of the fjord is negligible on the DIC pool. Overall, the fjord serves as a source of CO_2 to the atmosphere during the ice-free season, with an average yearly outgassing flux of 0.78 ± 0.16 mol·m^{-2}·yr^{-1}.

A study of the dissolved inorganic carbon budget of fjords not only affords information on their trophic status (i.e. source or sink of CO_2 with respect to the atmosphere) and surface-water chemistry, but also provides insights on the magnitude of gas exchange and the amount of biological activity it sustains. In addition to biological production, upwelling, water temperature, and the spreading of freshwater plumes all regulate pCO_2 in coastal systems. Wind speed is also critical as it impacts sea state and the efficiency of gas exchange at the air-sea interface (Chen et al., 2013). Hence, the importance of wind on controlling the CO_2 flux needs to be further investigated, especially in high latitude fjords where strong winds are often focussed along narrow channels between steep cliffs and narrow inlets.

Anthropogenic activities, through climate change, are altering the continental water cycle, along with the flows of carbon, nutrients and sediment to the coastal oceans (Borges, 2005), and therefore, the sequestration of anthropogenic CO_2 by the oceans. In glacial fjords, freshwater discharge will be modified by accelerated glacier melting and their ultimate demise. Knowledge of the spatial and temporal variability of glacial discharge and seasonal ice cover in high latitude fjords is essential to estimate their influence on circulation patterns and freshwater export, both of which impact local productivity, terrestrial carbon burial and export as well as CO_2 fluxes in these complex ecosystems. Finally, an improved understanding of the coastal carbon cycle will require a more comprehensive spatial and temporal coverage of surface mixed layer pCO_2 data in these environments, ideally from direct measurements.

Formatted: Font: Bold, English (United Kingdom)

Formatted: Indent: First line: 0 cm

Figures

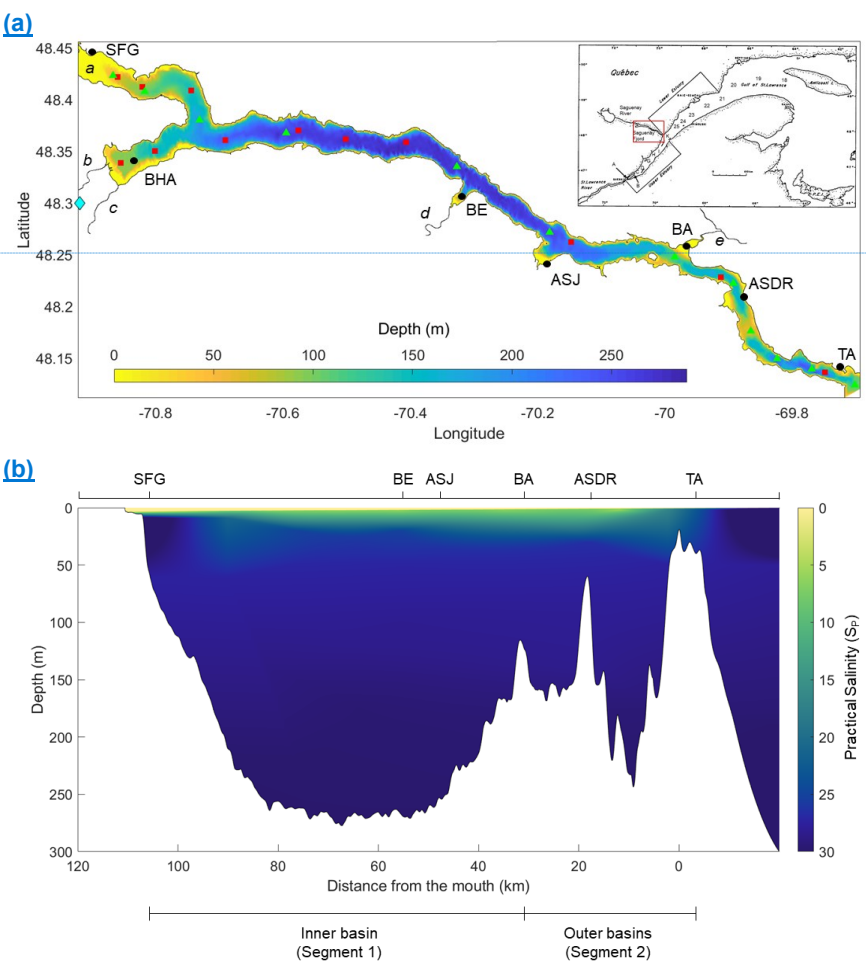

Figure 1. a) Bathymetry and geographic location of the Saguenay Fjord. Red ~~dots~~squares represent the hydrographic stations sampled during R/V Coriolis II cruises~~. b) Longitudinal section of~~ in September 2014, May 2016, June 2017 and May 2018. Green triangles represent the ~~Saguenay Fjord, showing~~hydrographic stations sampled during a SECO.net cruise onboard the ~~strong halocline.~~R/V Coriolis II in November 2017. The approximate ~~location~~locations of the following are shown: Tadoussac (TA), L'Anse de Roche (ASDR), Baie Sainte-Marguerite (BA), Anse-Saint-Jean (ASJ), Baie-Eternité (BE), St. ~~Fulgence (SF), Baie des Ha! Ha! (BHA).~~Fulgence (SFG), Baie des Ha! Ha! (BHA). The main tributaries to the fjord are also shown, including the Saguenay River (*a*), Rivière-à-Mars (*b*), Rivière des Ha! Ha! (*c*), Éternité River (*d*) and Sainte-Marguerite River (*e*). The blue diamond identifies the location of the La Baie weather station. Letters (A to K) and numbers (18 to 25) in the inset indicate the location of sampling stations in the St. Lawrence Estuary where data were acquired to define the SLRW, LSLE and CIL end-members. b) Longitudinal section along the Saguenay Fjord, showing the strong halocline.

Formatted: Font: Bold

Formatted: Normal

Formatted: Font: Helvetica, Font color: Auto

Commented [LD1]: Changes to figure:
Top panel
-Added tributaries *a, b, c, d*
-Changed inset map
-Added weather station location
-Differentiated stations location for ease of understanding in Appendix Fig. B
Bottom panel
-Added label "Practical Salinity (S_P)
-Added segments

Formatted: Font color: Black

Formatted: English (Canada)

(a)

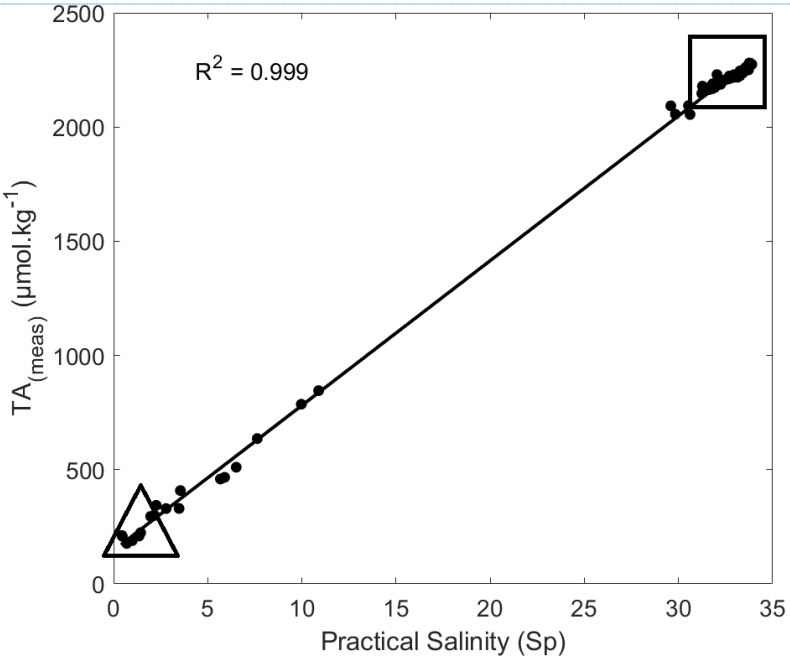

(b)

Saguenay River properties	
Practical salinity (S_P)	0.00 ± 0
$TA_{(meas)}$ (µmol·kg^{-1})	154 ± 52
$TA_{(calc)}$ (µmol·kg^{-1})	198 ± 51
Org Alk (µmol·kg^{-1})	-33 ± 3

Figure 2. a) Measured alkalinity ($TA_{(meas)}$) versus practical salinity (S_P) for SRW and CIL data points, for all sampling months (R^2 = ~~1~~0.999). The triangle defines the properties of the SRW, and the square comprises the properties of the CIL. b) $TA_{(meas)}$, $TA_{(calc)}$ and Org Alk definitions for the Saguenay River (SRW), using surface-water data from all sampling months, with standard error. The Org Alk (positive) contribution to the TA of the CIL is not considered as it accounts for less than 0.1 % of its TA.

Formatted: English (Canada)

Formatted Table

Formatted Table

Commented [LD2]: Changes to figure:
Top panel
-Modified R^2 to R^2 = 0.999 instead of 1

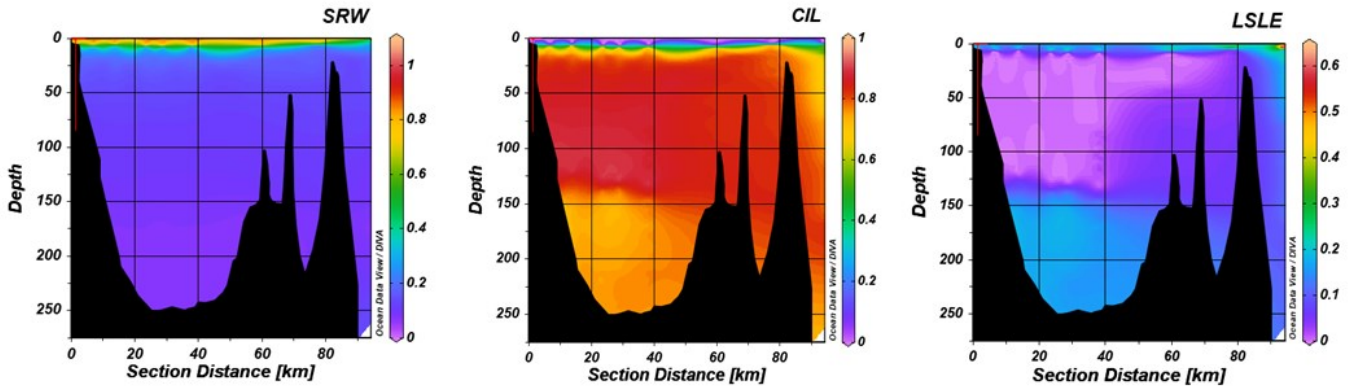

Figure 3. Vertical sections showing the relative contributions of the Saguenay River (SRW), the St. Lawrence Estuary Cold Intermediate Layer (CIL) and Lower St. Lawrence Estuary bottom waters (LSLE) to the water column structure of the Saguenay Fjord (June 2017). Fractions were estimated using an Optimum Multi-Parameter (OMP) algorithm (Tomczak and Large, 1989; Tomczak, 1981; Mackas and Harrison, 1997). A Variational Analysis (DIVA) interpolation was applied between field data points in Ocean Data View.

Formatted: Default Paragraph Font, Font: 9 pt

Formatted: Font: Times New Roman

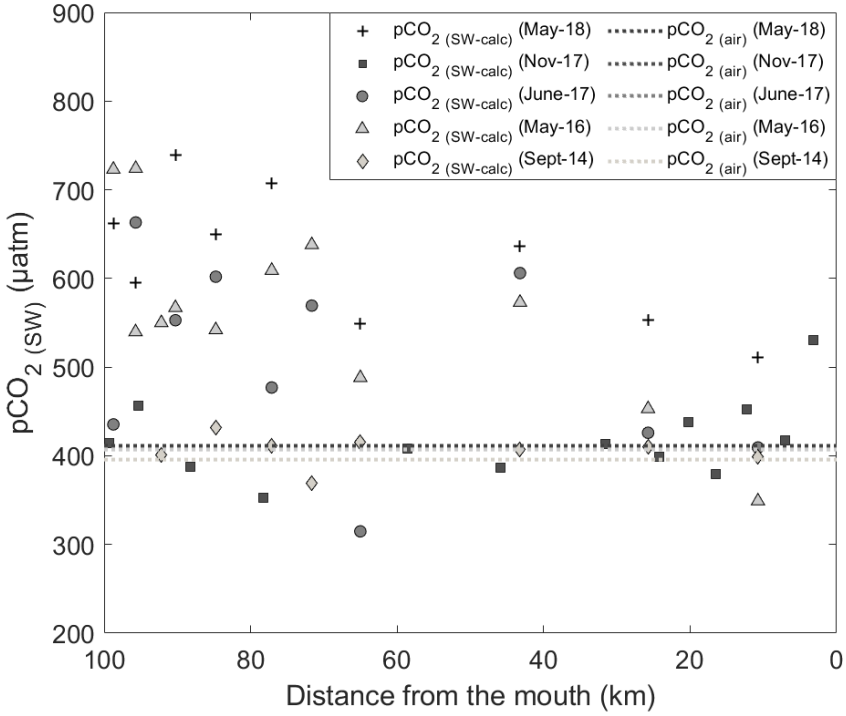

Figure 4. Spatial distribution of surface-water $pCO_{2(SW\text{-}calc)}$ in June 2017, November 2017, May 2016, September 2014 and May 2018. Dashed lines represent the $pCO_{2(air)}$ on the sampling months (respectively 396 ppm in September 2014, 407 ppm in May 2016, 408 ppm in June and November 2017, and 411 ppm in May 2018). Data points above the red line indicate that waters are sources of CO_2 to the atmosphere, whereas those below the red line identify waters that are sinks of atmospheric CO_2.

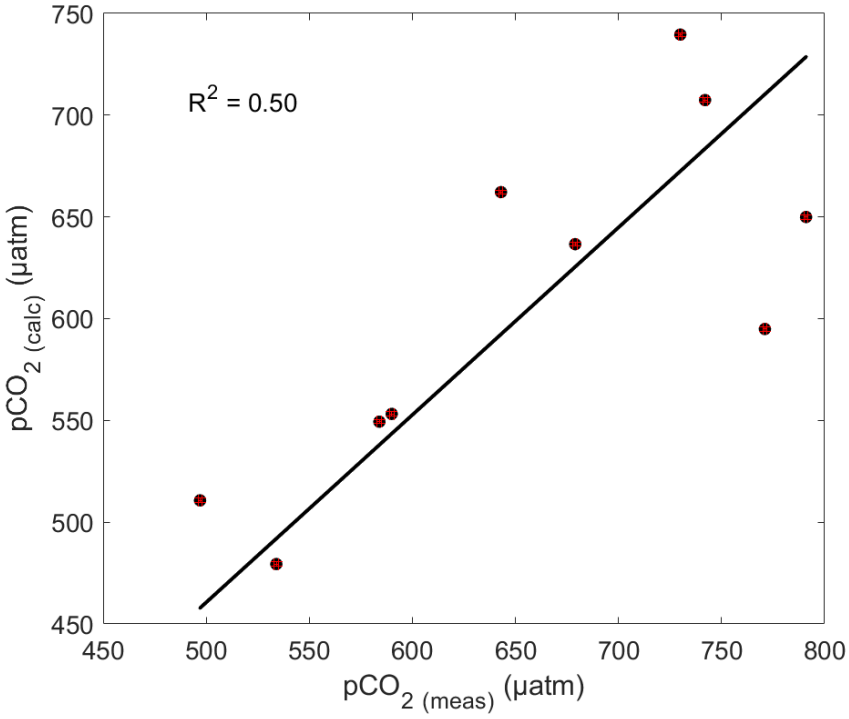

Figure 5. Correlation between $pCO_{2(SW-meas)}$ and $pCO_{2(SW-calc)}$ for May 2018. The black line shows the linear regression with a null intercept ($R^2 = 0.50$). Error bars, in red, are smaller than the symbol.

Commented [LD3]: Changes to figure:
-Added error bars (both vertical and horizontal)

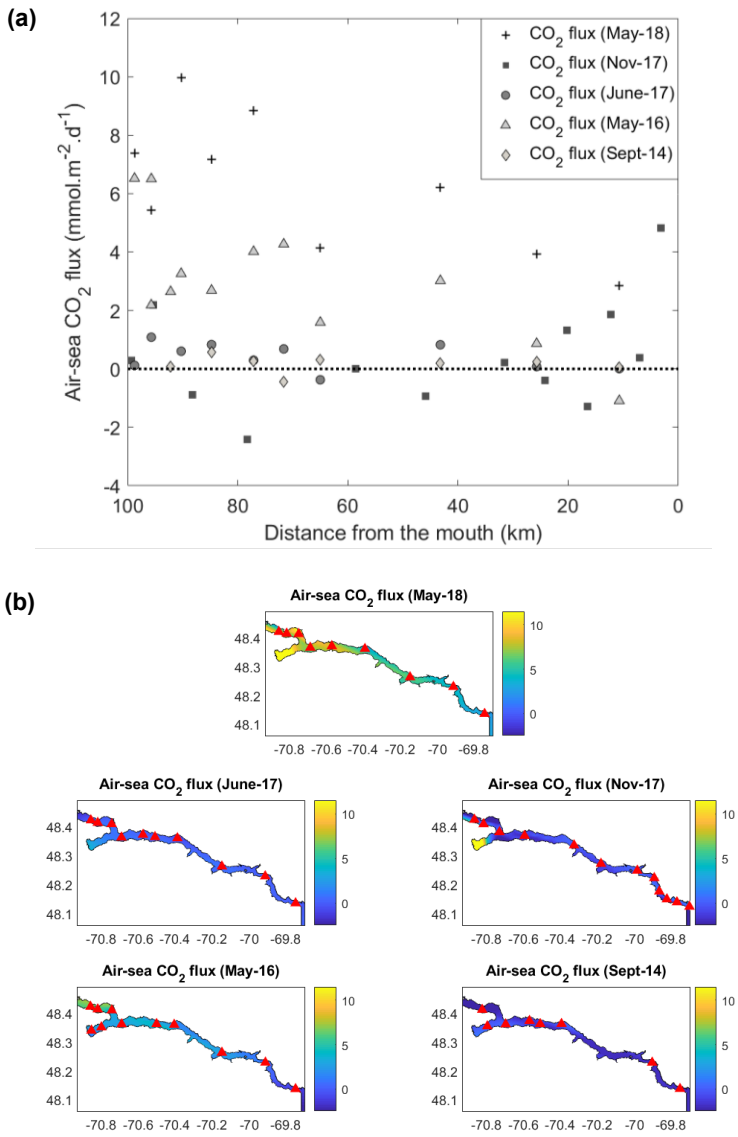

Figure 6. a) Spatial distribution of air-sea CO_2 flux (mmol·m^{-2}·d^{-1}) in the Saguenay Fjord for all cruises. Data points above the ~~red~~dashed line indicate sources of CO_2 to the atmosphere, whereas those below the red line are sinks of atmospheric CO_2; b) Spatial interpolation of air-sea CO_2 fluxes (mmol·m^{-2}·d^{-1}) in the Saguenay Fjord for all cruises. Red triangles ~~indicate~~identify sampling locations.

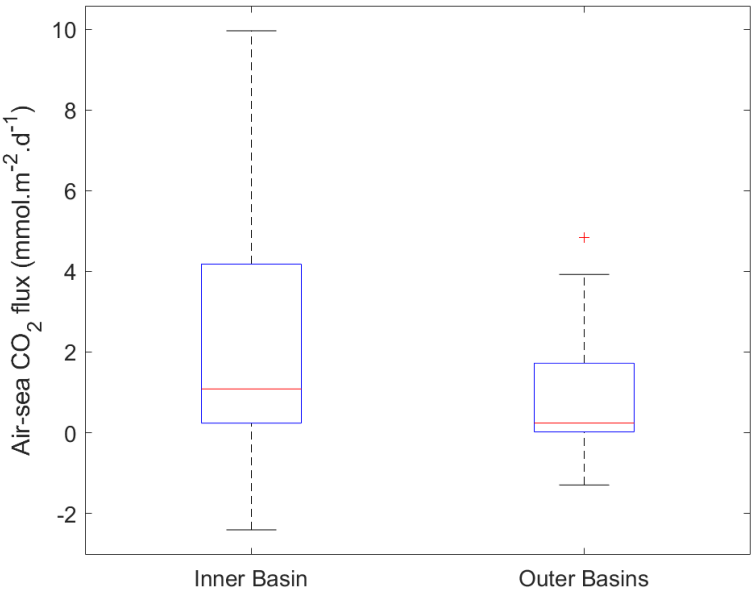

Figure 7. Box-plot of the air-sea CO_2 fluxes from all data in the two subsections of the study area (Inner basin and Outer basins). The red line is the median, the box spans the interquartile range (25-75 percentiles) and the whiskers show the extreme data points not considered outliers. One outlier is identified by the red + symbol.

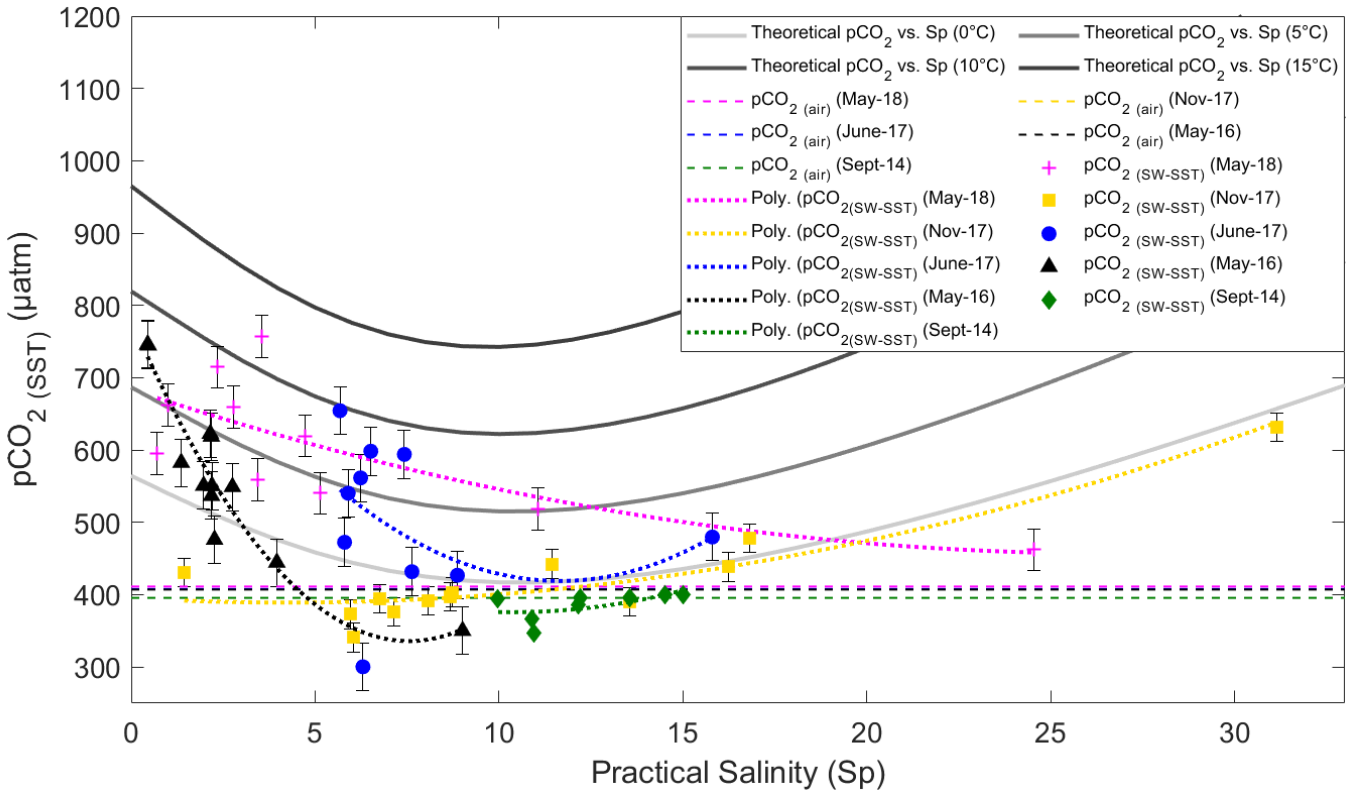

Figure 8. Temperature-normalized field $pCO_{2(SW\text{-}SST)}$, and results of the conservative, two end-member mixing model for $pCO_{2(SW\text{-}SST)}$ in the Saguenay Fjord surface waters. $pCO_{2(SW\text{-}calc)}$ were normalized at each station to the average surface water temperature per sampling month (i.e., T = 10.4°C for September 2014, T = 5.04°C for May 2016, T = 11.9°C for June 2017, T = 7.13°C for November 2017 and T = 5.08°C for May 2018) to account for the effects of temperature on the CO_2 solubility in water, following the procedure described in Jiang et al. (2008). Dashed lines represent the $pCO_{2(air)}$ on the sampling months (396 ppm in September 2014, 407 ppm in May 2016, 408 ppm in June and November 2017, and 411 ppm in May 2018). Error bars show standard error of the mean for $pCO_{2(SW\text{-}SST)}$ values – bars are smaller than the symbol for September 2014.

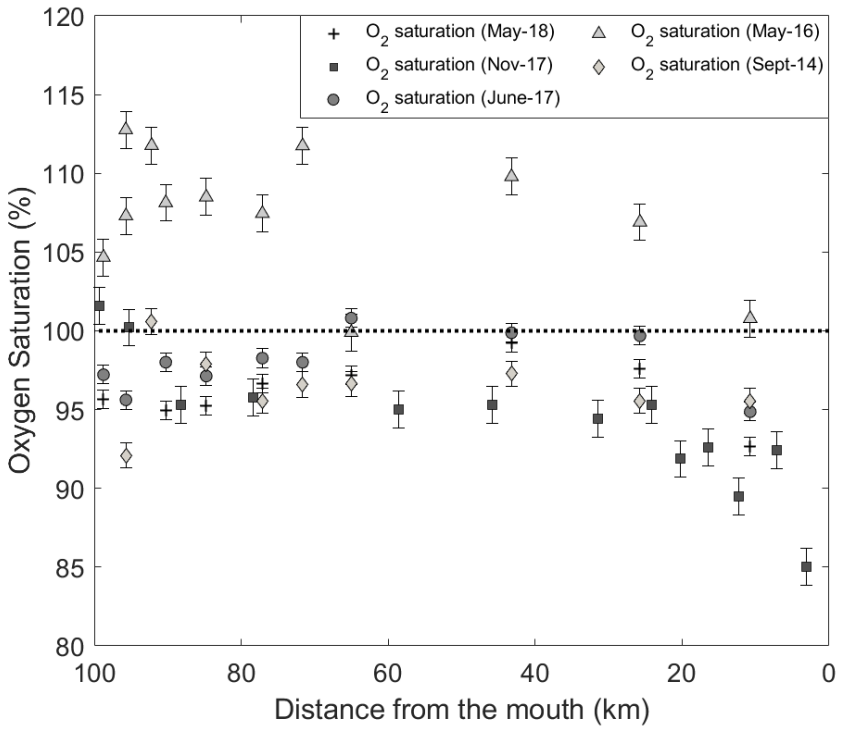

Figure 9. Spatial distribution of surface-water dissolved O_2 saturation (%) in May 2018, June 2017, November 2017, May 2016 and September 2014. The dashed line represents equilibrium with the atmosphere (i.e., 100% saturation). Data points above the line indicate that waters are supersaturated in O_2, whereas those below the line identify O_2-undersaturated waters with respect to the atmosphere. Error bars show standard error of the mean for O_2 saturation values.

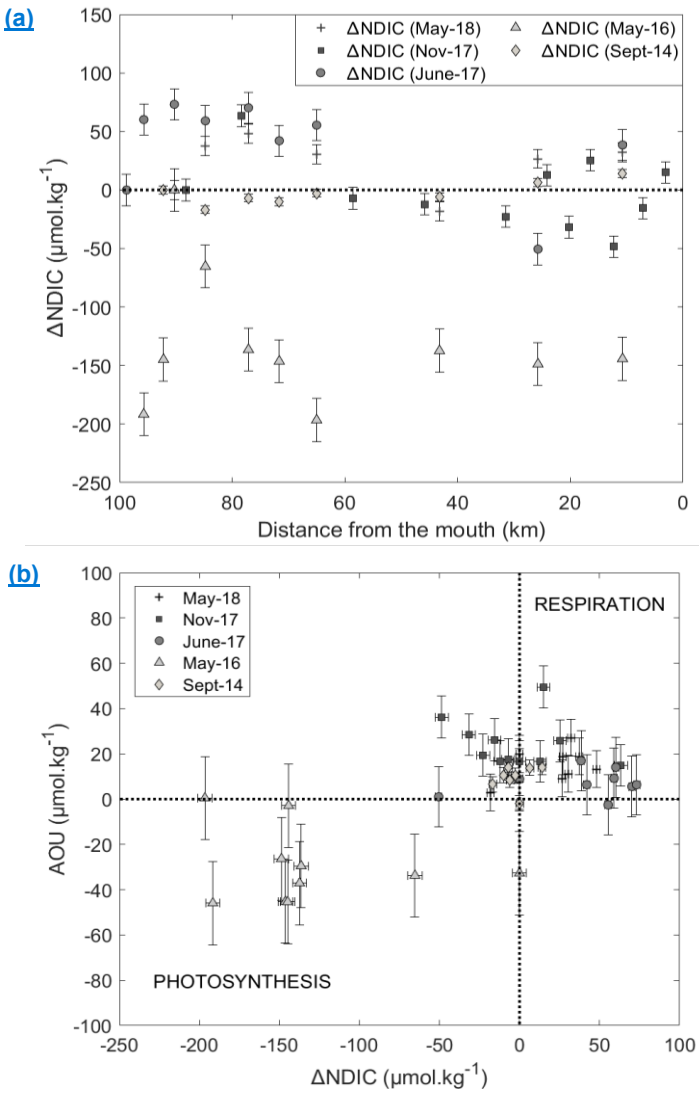

Figure 10. a) ΔNDIC (i.e. change in NDIC relative to the saline waters at the head of the fjord) distribution in the Saguenay Fjord surface waters. Data were normalized to a common salinity (average for each sampling period) according to the method of Friis *et al.* (2003); Error bars show standard error of the mean for NDIC values. b) Apparent oxygen utilization (AOU) against ΔNDIC. Error bars show standard error of the mean for AOU values.

Tables

SWT	Salinity	Temperature (°C)	$TA_{(meas)}$ (µmol·kg^{-1})	$\delta^{18}O$ (per mil)	DIC (µmol·kg^{-1})	DO (µmol·L^{-1})
SRW	0.00 ± 0	6.19 ± 0.18	154 ± 13	-12.17 ± 0.21	230 ± 12	411 ± 6
CIL	32.52 ± 0.05	1.44 ± 0.08	2210 ± 2	-1.12 ± 0.03	2141 ± 3	256 ± 5
LSLE	34.31 ± 0.01	5.16 ± 0.18	2294 ± 2	-0.17 ± 0.02	2276 ± 3	76 ± 1
SLRW	0.00 ± 0	12.11 ± 0.13	1099 ± 16	-8.09 ± 0.13	1140 ± 15	329 ± 5
Weights	25	1	25	25	15	1

Formatted Table

Formatted Table

Table 1. Source-Water Type (SWT) definitions for the Saguenay River (SWR), the St. Lawrence Estuary summertime Cold Intermediate Layer (CIL), the Lower St. Lawrence Estuary bottom water (LSLE) and the St. Lawrence River (SLRW). Definitions and variances were derived from data taken in September 2014, May 2016, June 2017 and November 2017. Data for SRW and SLRW were extrapolated to $S_P = 0$. The weights used in the OMP analysis are also shown.

Sampling Month	$pCO_{2(SW-calc)}$ (µatm)	k (cm h^{-1})	u (m s^{-1})	F (mmol·m^{-2}·d^{-1})
May 2018	623 ± 26 (511/740)	1.94 ± 0.01 (1.89/1.97)	3.91	6.2 ± 0.79 (2.9/10.0)
November 2017	418 ± 12 (353/530)	3.2 ± 0.04 (2.82/3.38)	4.2	0.40 ± 0.51 (-2.4/4.8)
June 2017	506 ± 35 (315/663)	0.37 ± 0.01 (0.36/0.42)	1.89	0.42 ± 0.15 (-0.4/1.1)
May 2016	563 ± 31 (349/724)	1.26 ± 0.01 (1.15/1.30)	3.17	3.04 ± 0.62 (-1.1/6.5)
September 2014	406 ± 6 (369/432)	1.43 ± 0.01 (1.39/1.49)	3.71	0.16 ± 0.10 (-0.43/0.56)

Formatted Table

Formatted Table

Table 2. Mean, standard error of the mean and range of $pCO_{2(SW)}$, k, u and F in the Saguenay Fjord surface waters. Numbers in parentheses indicate the observed or calculated ranges. Overall, the total area-averaged degassing flux of the fjord adds up to 2.14 ± 0.43 mmol·m^{-2}·d^{-1} ~~(i.e.~~or 0.78 ± 0.16 mol·m^{-2}·yr^{-1}~~).~~.

Data availability

Data presented in this paper are available upon request from one of the authors (louise.delaigue@mail.mcgill.ca).

Appendix

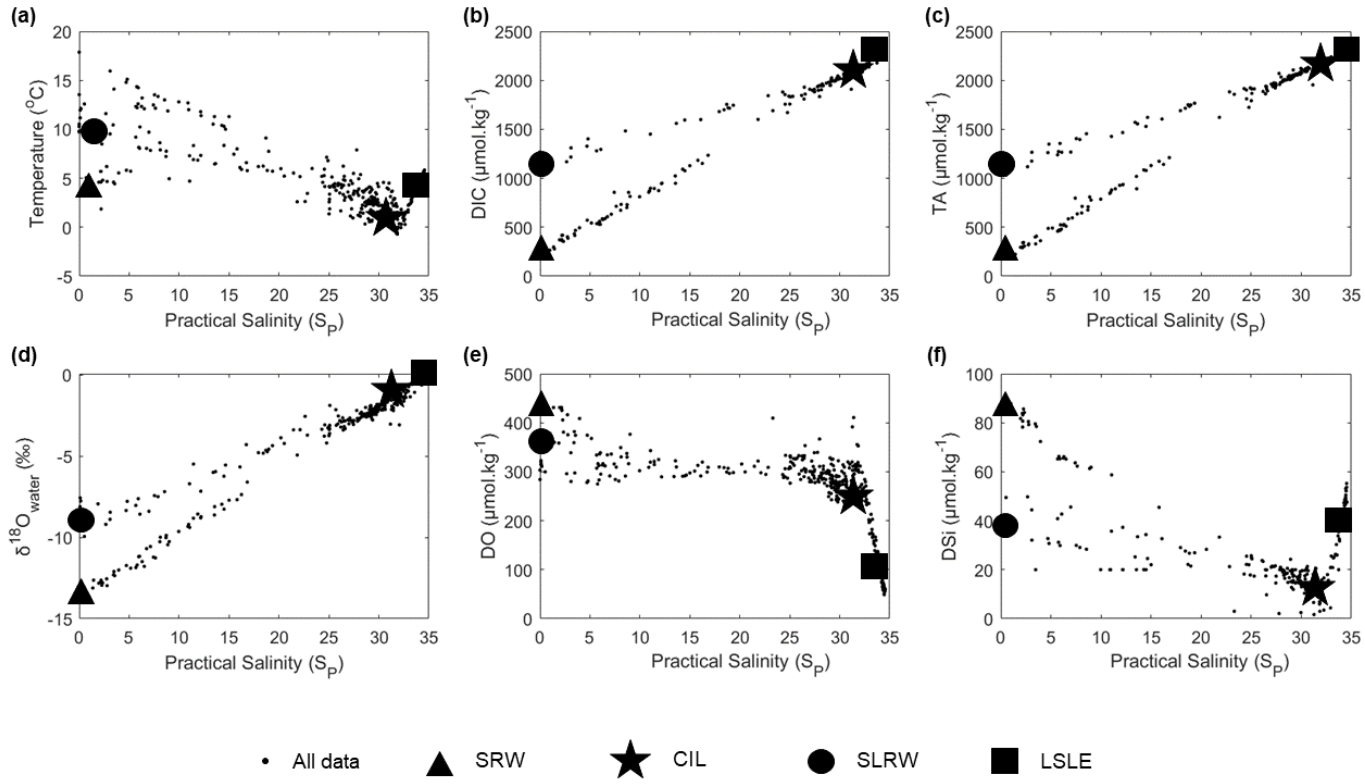

Figure A. a) Temperature, b) Dissolved Inorganic Carbon (DIC), c) Total Alkalinity (TA), d) δ^{18}Owater, e) Dissolved Oxygen (DO), and f) Dissolved silicate (DSi) versus practical salinity (SP) for ~~data from~~samples collected in September 2014, May 2016, June 2017, November 2017 and May 2018. Each large symbol (square, circle, triangle and star) ~~represents~~identifies distinct source ~~-~~water masses.

Formatted: Superscript

Sampling months / Stations	Distance from the mouth (km)	Sept-14		May-16		June-17		May-18	
		pH_{NBS}	pH_T	pH_{NBS}	pH_T	pH_{NBS}	pH_T	pH_{NBS}	pH_T
St-Fulgence	98.7	-	-	7.348	-	7.782	-	7.171	
SAG-02 (BHA)	95.7	-	-	7.429	-	-	-	-	
SAG-05	95.7	-	7.598	7.126	-	7.478	-	7.219	
SAG-06	90.3	-	-	7.118	-	7.559	-	-	7.201
SAG-09 (BHA)	92.2	-	7.733	7.273	-	-	-	-	-
SAG-15	84.8	-	7.682	7.194	-	-	7.413	-	7.187
SAG-20	77.1	-	7.753	7.288	-	-	7.484	-	7.111
SAG-25	71.7	-	7.772	7.348	-	-	7.440	-	-
SAG-30	65.0	-	7.801	7.439	-	-	7.703	-	7.309
SAG-36	43.2	-	7.758	7.351	-	-	7.574	-	7.359
SAG-42	25.7	-	7.780	7.483	7.330	-	7.714	-	7.394
SAG-48	10.7	-	7.805	7.863	7.690	-	7.819	-	7.604

Figure B.1 Raw in-situ pH data for surface waters collected in September 2014, May 2016, June 2017 and May 2018. Where possible, pH is reported on the total scale, except for freshwater samples which are reported on the NBS scale. No pH data is available on the NBS scale for September 2014 as $10.0 < S_P < 12.4$. Few pH data are available on the total scale for May 2016 as $0.45 < S_P < 9.0$.

Stations	Distance from the mouth (km)	Nov-17	
		pH_{NBS}	pH_T
SAG-01	3.12	-	7.862
SAG-02	7.00	-	7.784
SAG-03	12.3	-	7.777
SAG-04	16.5	-	7.755
SAG-05	20.3	-	7.679
SAG-06	24.2	-	7.632
SAG-07	31.5	-	7.637
SAG-08	45.9	-	7.616
SAG-09	58.6	-	7.579
SAG-10	78.3	-	7.589
SAG-11	88.3	-	7.573
SAG-12	95.3	-	7.251
SAG-13	99.3	-	7.608

Figure B.2 Raw in-situ pH data for surface waters collected in November 2017. pH was only reported on the total scale during this cruise, where $1.4 < S_P < 31.2$.

Author contribution

A.M. and L.D. conceived the project. A.M. acquired and processed the data prior to 2016. L.D. conducted the data analysis and wrote the first draft of the paper whereas A.M. provided editorial and scientific recommendations. H.T. provided results of alkalinity and dissolved inorganic carbon analyses and scientific recommendations.

Competing interests

The authors declare that they have no conflict of interest.

Acknowledgements

We would like to give special thanks to Gilles Desmeules as well as the Captains and crew of the R/V Coriolis II without whom, over the years, this project would not have been possible. Most of the data presented in this study were acquired opportunistically on research cruises funded by Ship-Time Program grants to A.M. or Canadian colleagues by the Natural Sciences and Engineering Research Council of Canada (NSERC). The work was funded by a Regroupement Stratégique grant from the Fonds Québécois de Recherche Nature et Technologies (FQRNT) to GEOTOP as well as NSERC Discovery and Marine Environmental Observation, Prediction and Response Network (MEOPAR; Canadian Ocean Acidification Research partnership) grants to A.M and H.T. We would like to thank Dr. Jean-Francois Hélie at GEOTOP-UQAM for carrying out the $\delta^{18}O_{water}$ analyses as well as Constance Guignard for cruise preparation and support in the laboratory. Finally, L.D. wishes to thank MEOPAR and the Department of Earth and Planetary Sciences at McGill for financial support in the form of stipends, scholarships and assistantships. Bathymetric data of the fjord were graciously provided by Mélanie Belzile. Figure (3) in this study was created with the Ocean Data View Software (Schlitzer, ~~2015~~2002).

References

Annane, S., St-Amand, L., Starr, M., Pelletier, E., and Ferreyra, G. A.: Contribution of transparent exopolymeric particles (TEP) to estuarine particulate organic carbon pool, Mar. Ecol. Prog. Ser., 529, 17-34, 2015.

Bauer, J. E., Cai, W. J., Raymond, P. A., Bianchi, T. S., Hopkinson, C. S., and Regnier, P. A.: The changing carbon cycle of the coastal ocean, Nature, 504, 61-70, 2013.

Bélanger, C.: Observation and modelling of a renewal event in the Saguenay Fjord, Ph.D thesis, Université du Québec à Rimouski, Que., Canada, 2003.

Bellis, A.: Spectrophotometric determination of pH in estuarine waters using Phenol Red, B. Sc. thesis, McGill University, Montreal, Que., Canada, 53 pp., 2002.

Belzile, M., Galbraith, P. S., and Bourgault, D.: Water renewals in the Saguenay Fjord, J. Geophys. Res-Oceans, 121, 638-657, 2016.

Borges, A. V.: Do we have enough pieces of the jigsaw to integrate CO_2 fluxes in the coastal ocean?, Estuaries, 28(1), 3-27, 2005.

Bourgault, D., Galbraith, P. S., and Winkler, G.: Exploratory observations of winter oceanographic conditions in the Saguenay Fjord, Atmos. -Ocean, 50, 17-30, 2012.

Brewer, P. G., and Peltzer, E. T.: Limits to marine life, Science, 324, 347-348, 2009.

Cai, W. J.: Estuarine and coastal ocean carbon paradox: CO_2 sinks or sites of terrestrial carbon incineration?, Annu. Rev. Mar. Sci., 3(1), 123-145, 2011.

Cai, W. J., and Wang, Y.: The chemistry, fluxes, and sources of carbon dioxide in the estuarine waters of the Satilla and Altamaha Rivers, Georgia, Limnol. Oceanogr., 43, 657-668, 1998.

Cai, W. J., Wang, Y., and Hodson, R. E.: Acid-base properties of dissolved organic matter in the estuarine waters of Georgia, USA, Geochim Cosmochim. Acta, 62, 473-483, 1998.

Caldeira, K., and Wickett, M. E.: Ocean model predictions of chemistry changes from carbon dioxide emissions to the atmosphere and ocean, J. Geophys. Res-Oceans, 110, 2005.

Chassé, R., and Côté, R.: Aspects of winter primary production in the upstream section of Saguenay Fjord, Hydrobiologia, 215, 251-260, 1991.

Chen, C. T. A., & Borges, A. V.: Reconciling opposing views on carbon cycling in the coastal ocean: Continental shelves as sinks and near-shore ecosystems as sources of atmospheric CO_2, Deep-Sea Res. Pt. II, 56(8-10), 578-590, 2009.

Chen, C. T., Huang, T. H., Chen, Y. C., Bai, Y., He, X., and Kang, Y.: Air–sea exchanges of CO_2 in the world's coastal seas, Biogeosciences, 10(10), 6509-6544, 2013.

Chester, R. (Eds.): Marine Geochemistry, Springer, Netherlands, 702 pp., 1990.

Clayton, T. D., and Byrne, R. H.: Spectrophotometric seawater pH measurements: total hydrogen ion concentration scale calibration of m-cresol purple and at-sea results, Deep-Sea Res. Pt. I, 40, 2115-2129, 1993.

Dickie, L. M. and Trites, R. W.: The Gulf of St. Lawrence, in: Estuaries and Enclosed Seas, Ecosystems of the World 26, edited by: Ketchum, B. H., Elsevier, 403-425, 1983.

Dickson, A. G., Sabine, C. L., and Christian, J. R.: Guide to Best Practices for Ocean CO_2 Measurements, PICES Special Publication 3, 191 pp., Sidney, BC, Canada, 2007.

Dinauer, A., and Mucci, A.: Spatial variability in surface-water pCO_2 and gas exchange in the world's largest semi-enclosed estuarine system: St. Lawrence Estuary (Canada), Biogeosciences, 14, 3221-3237, 2017.

Dinauer, A., and Mucci, A.: Distinguishing between physical and biological controls on the spatial variability of pCO_2: A novel approach using OMP water mass analysis (St. Lawrence, Canada), Mar. Chem., 204, 107-120, 2018.

Doney, S. C., Fabry, V. J., Feely, R. A., and Kleypas, J. A.: Ocean acidification: The Other CO_2 Problem, Ann. Rev. Mar. Sci., 1, 169–192, 2009.

Douglas, N. K., and Byrne, R. H.: Achieving accurate spectrophotometric pH measurements using unpurified meta-cresol purple, Mar. Chem., 190, 66-72, 2017.

El-Sabh, M. I., and Silverberg, N.: The St. Lawrence Estuary: Introduction, in: Oceanography of a Large-Scale Estuarine System, edited by: El-Sabh, M. I. and Silverberg, N., Springer-Verlag, New York, NY, 1-9, 1990.

Epstein, S., and Mayeda, T.: Variation of O^{18} content of waters from natural sources, Geochim. Cosmochim. Acta, 4, 213-224, 1953.

Feely, R. A.: Impact of Anthropogenic CO_2 on the $CaCO_3$ System in the Oceans, Science, 305, 362-366, 2004.

Friis, K., Körtzinger, A., and Wallace, D. W.: The salinity normalization of marine inorganic carbon chemistry data, Geophys. Res. Lett., 30, 2003.

Frankignoulle, M.: Field measurements of air-sea CO_2 exchange 1, Limnol. Oceanogr., 33(3), 313-322, 1988.

Galbraith, P. S.: Winter water masses in the Gulf of St. Lawrence, J. Geophys. Res-Oceans, 111, C06022, 2006.

Gattuso, J.-P., Frankignoulle, M., and Wollast, R.: Carbon and carbonate metabolism in coastal aquatic ecosystems, Annu. Rev. Ecol. Syst., 29, 405-434, 1998.

Gilbert, D., and Pettigrew, B.: Interannual variability (1948-1994) of the CIL core temperature in the Gulf of St. Lawrence, Can. J. Fish. Aquat. Sci., 54, 57-67, 1997.

Grasshoff, K., Kremling, K., and Ehrhardt, M. (Eds.): Methods of Seawater Analysis 3rd Edn., Wiley-VCH, Weinheim, Germany, 1999.

Gratton, Y., Mertz, G., and Gagné, J. A.: Satellite observations of tidal upwelling and mixing in the St. Lawrence Estuary, J. Geophys. Res-Oceans, 93, 6947-6954, 1988.

Hönisch, B., Ridgwell, A., Schmidt, D.N., Thomas, E., Gibbs, S.J., Sluijs, A., Zeebe, R., Kump, L., Martindale, R.C., Greene, S.E. and Kiessling, W.: The geological record of ocean acidification, Science, 335, 1058-1063, 2012.

Hunt, C. W., Snyder, L., Salisbury, J. E., Vandemark, D., and McDowell, W. H.: SIPCO_2: A simple, inexpensive surface water pCO_2 sensor, Limnol. Oceanogr-Meth., 15, 291-301, 2017.

Jiang, L. Q., Cai, W. J., and Wang, Y.: A comparative study of carbon dioxide degassing in river-and marine dominated estuaries, Limnol. Oceanogr., 53, 2603-2615, 2008.

Juul-Pedersen, T., Arendt, K., Mortensen, J., Blicher, M., Søgaard, D., and Rysgaard, S.: Seasonal and interannual phytoplankton production in a sub-Arctic tidewater outlet glacier fjord, SW Greenland, Mar. Ecol. Prog. Ser., 524, 27-38, 2015.

Karstensen, J.: OMP (Optimum Multiparameter) analysis - USER GROUP. Retrieved from http://omp.geomar.de/, 2013.

Karstensen, J., and Tomczak, M.: Age determination of mixed water masses using CFC and oxygen data, J. Geophys. Res-Oceans, 103, 18599-18609, 1998.

Ko, Y. H., Lee, K., Eom, K. H., and Han, I. S.: Organic alkalinity produced by phytoplankton and its effect on the computation of ocean carbon parameters, Limnol. Oceanogr., 61, 1462-1471, 2016.

Lansard, B., Mucci, A., Miller, L. A., Macdonald, R. W., and Gratton, Y.: Seasonal variability of water mass distribution in the southeastern Beaufort Sea determined by total alkalinity and $\delta^{18}O$, J. Geophys. Res-Oceans, 117, 2012.

Lavoie, D., Starr, M., Zakardjian, B., & Larouche, P. : Identification of ecologically and biologically significant areas (EBSA) in the Estuary and Gulf of St. Lawrence: Primary production, Fisheries and Oceans, 2008.

Le Quéré, C., Andres, R. J., Boden, T., Conway, T., Houghton, R. A., House, J. I., Marland, G., Peters, G. P., van der Werf, G. R., Ahlstrom, A., Andrew, R. M., Bopp, L., Canadell, J. G., Ciais, P., Doney, S.C., Enright, C.M., Friedlingstein, P., Huntingford, C., Jain, A. K., Jourdain, C., Kato, E., Keeling, R. F., Klein Goldewijk, K., Levy, S., Levy, P., Lomas, M., Poulter, B., Raupach, M. R., Schwinger, J., Sitch, S., Stocker, B. D., Viovy, N., Zaehle, S. and Zeng, N.: The global carbon budget 1959–2011, Earth Syst. Sci. Data, 5(2), 1107-1157, 2012.

Levasseur, M. E., and Therriault, J. C.: Phytoplankton biomass and nutrient dynamics in a tidally induced upwelling: the role of the NO3: SiO4 ratio, Mar. Ecol. Prog. Ser, 39, 87-97, 1987.

Lueker, T. J., Dickson, A. G., and Keeling, C. D.: Ocean pCO_2 calculated from dissolved inorganic carbon, alkalinity, and equations for K_1 and K_2: validation based on laboratory measurements of CO_2 in gas and seawater at equilibrium, Mar. Chem., 70, 105-119, 2000.

~~Lüthi, D., Le Floch, M., Bereiter, B., Blunier, T., Barnola, J.M., Siegenthaler, U., Raynaud, D., Jouzel, J., Fischer, H., Kawamura, K. and Stocker, T.F.: High-resolution carbon dioxide concentration record 650,000–800,000 years before present, Nature, 453, 2008.~~

Mackas, D. L., Denman, K. L., and Bennett, A. F.: Least squares multiple tracer analysis of water mass composition, J. Geophys. Res-Oceans, 92, 2907-2918, 1987.

Mackas, D. L., and Harrison, P. J.: Nitrogenous nutrient sources and sinks in the Juan de Fuca Strait/Strait of Georgia/Puget Sound estuarine system: assessing the potential for eutrophication, Estuar. Coast Shelf Sci., 44, 1-21, 1997.

Formatted: English (Canada)

Millero, F. J.: The pH of estuarine waters, Limnol. Oceanogr., 31, 839-847, 1986.

Mucci, A., Levasseur, M., Gratton, Y., Martias, C., Scarratt, M., Gilbert, D., Tremblay, J.É., Ferreyra, G. and Lansard, B.: Tidally induced variations of pH at the head of the Laurentian Channel, Can. J. Fish. Aquat. Sci., 75, 1128-1141, 2017.

~~Mucci, A.,~~ Najjar R. G., Herrmann M., Alexander R., Boyer E. W., Burdige D. J., Butman D., Cai W. J.,Canuel E. A., Chen R. F., Friedrichs M. A. M., Feagin R. A., Griffith P. C., Hinson A. L.,Holmquist J. R., Hu X., Kemp W. M., Kroeger K. D., Mannino A., McCallister S. L.,McGillis W. R., Mulholland M. R., Pilskaln C. H., Salisbury J., Signorini S. R.,St-Laurent P., Tian H., Tzortziou M., Vlahos P., Wang Z. A. and Zimmerman R. C.: Carbon budget of tidal wetlands, estuaries, and shelf waters of eastern North America, Global Biogeochem. Cy., 32, 389-416, 2018.

~~Starr, M., Gilbert, D., and Sundby, B.: Acidification of lower St. Lawrence Estuary bottom waters, Atmos. Ocean, 49, 206-218, 2011.~~

Orr, J. C.: Recent and future changes in ocean carbonate chemistry, in: Ocean acidification, edited by: Gattuso, J.-P. and Hansson, L., Oxford University Press, Oxford, UK, 1, 25 pp., 2011.

Pierrot, D., Lewis, E., and Wallace, D. W. R.: MS Excel Program Developed for CO_2 System Calculations, ORNL/CDIAC-105a, Carbon Dioxide Information Analysis Center, Oak Ridge National Laboratory, U.S. Department of Energy, Oak Ridge, Tennessee, 2006.

Piper, D. J. W., Mudie, P. J., Fader, G. B., Josenhans, H. W., MacLean, B., and Vilks, G.: Quaternary Geology, Chapter 10, in: Geology of the Continental Margin of Eastern Canada (Vol. 2), Geological Survey of Canada, edited by: Keen, M. J. and William, G. L., Canada, 1990.

Rhein, M., Rintoul, S.R., Aoki, S., Campos, E., Chambers, D., Feely, R.A., Gulev, S., Johnson, G.C., Josey, S.A., Kostianoy, A., Mauritzen, C., Roemmich, D., Talley, L.D., and Wang, F.: Observations: Ocean, in: Climate Change 2013: The Physical Science Basis, Contribution of Working Group I to the Fifth Assessment Report of the Intergovernmental Panel on Climate Change, edited by: Stocker, T.F., Qin, D., Plattner, G.-K., Tignor, M., Allen, S.K., Boschung, J., Nauels, A., Xia, Y., Bex, V. and Midgley, P.M., Cambridge University Press, Cambridge, United Kingdom and New York, NY, USA, 2013.

Robert-Baldo, G. L., Morris, M. J., and Byrne, R. H.: Spectrophotometric determination of seawater pH using phenol red, Anal. Chem., 57, 2564-2567, 1985.

Formatted: English (Canada)

Rysgaard, S., Mortensen, J., Juul-Pedersen, T., Sørensen, L. L., Lennert, K., Søgaard, D. H., Arendt, K. E., Blicher, M. E., Sejr, M. K. and Bendtsen, J.: High air–sea CO_2 uptake rates in nearshore and shelf areas of Southern Greenland: Temporal and spatial variability, Mar. Chem., 128-129, 26-33, 2012.

Sabine, C. L.: The oceanic sink for anthropogenic CO_2, Science, 305(5682), 367-371, 2004.

Saucier, F. J., and Chassé, J.: Tidal circulation and buoyancy effects in the St. Lawrence Estuary, Atmos.Ocean, 38, 505-556, 2000.

Schlitzer, R.: Interactive analysis and visualization of geoscience data with Ocean Data View. Computers & geosciences, 28(10), 1211-1218, 2002.

Seibert, G. H., Trites, R. W., and Reid, S. J.: Deepwater exchange processes in the Saguenay Fjord, J. Fish. Board Can., 36(1), 42– 53, 1979.

Smith, J. N., and Walton, A.: Sediment accumulation rates and geochronologies measured in the Saguenay Fjord using the Pb-210 dating method, Geochim. Cosmochim. Acta, 44, 225-240, 1980.

Smith, R. W., Bianchi, T. S., Allison, M., Savage, C., and Galy, V.: High rates of organic carbon burial in fjord sediments globally, Nat. Geosci., 8(6), 450-453, 2015.

Stacey, M. W., and Gratton, Y.: The energetics and tidally induced reverse renewal in a two-silled fjord, J.Phys. Oceanogr., 31, 1599-1615, 2001.

Telmer, K., and Veizer, J.: Carbon fluxes, pCO_2 and substrate weathering in a large northern river basin, Canada: carbon isotope perspectives, Chem. Geol., 159, 61-86, 1999.

Therriault, J. C., and Lacroix, G.: Penetration of the deep layer of the Saguenay Fjord by surface waters of the St. Lawrence Estuary, Journal of the Fisheries Board of Canada, 32, 2373-2377, 1975.

Tomczak Jr, M.: An analysis of mixing in the frontal zone of South and North Atlantic Central Water off North-West Africa, Prog. Oceanogr., 10, 173-192, 1981.

Tomczak, M.: Potential vorticity as a tracer in quantitative water mass analysis, International WOCE Newsletter, 36, 6-10, 1999.

Tomczak, M., and Large, D. G.: Optimum multiparameter analysis of mixing in the thermocline of the eastern Indian Ocean, J. Geophys. Res-Oceans, 94, 16141-16149, 1989.

Tremblay, L., and Gagné, J. P.: Organic matter distribution and reactivity in the waters of a large estuarine system, Mar. Chem., 116, 1-12, 2009.

Wanninkhof, R.: Relationship between wind speed and gas exchange over the ocean, J. Geophys. Res Oceans, 97, 7373-7382, 1992.

Wanninkhof, R.: Relationship between wind speed and gas exchange over the ocean revisited, Limnol. Oceanogr.-Meth., 12, 351-362, 2014.

Wanninkhof, R.~~: Relationship between wind speed and gas exchange over the ocean.~~, and Triñanes, J.: The impact of changing wind speeds on gas transfer and its effect on global air-sea CO_2 fluxes, Global Biogeochem. Cy., 31(6), 961-974, 2017.

~~, J. Geophys. Res Oceans, 97, 7373-7382, 1992.~~

Weiss, R.: Carbon dioxide in water and seawater: the solubility of a non-ideal gas, Mar. Chem., 2, 203-215, 1974.

Weiss, R. F., and Price, B. A.: Nitrous oxide solubility in water and seawater, Mar. Chem., 8, 347-359, 1980.

Willeit, M., Ganopolski, A., Calov, R., & Brovkin, V.: Mid-Pleistocene transition in glacial cycles explained by declining CO_2 and regolith removal, Science Advances, 5(4), eaav7337, 2019.

Xie, H., Aubry, C., Bélanger, S., and Song, G.: The dynamics of absorption coefficients of CDOM and particles in the St. Lawrence estuarine system: Biogeochemical and physical implications, Mar. Chem., 128, 44-56, 2012.

Zakardjian, B. A., Gratton, Y., and Vézina, A. F.: Late spring phytoplankton bloom in the Lower St. Lawrence Estuary: the flushing hypothesis revisited, Mar. Ecol. Prog. Ser., 192, 31-48, 2000.

Zeebe, R. E., and Wolf-Gladrow, D. (Eds.): CO_2 in seawater: equilibrium, kinetics, isotopes, Elsevier Oceanography Series 65, Amsterdam, 2001.